Synthesis, Characterization, and Thermotropic Properties of Side-Chain Liquid Crystalline Polysiloxane Polymers with an Oligo(ethylene oxide) Unit in the Side Chain

GUO-PING CHANG-CHIEN[1,*] and JEN-FENG KUO[2]

[1] Department of Chemical Engineering, Cheng-Shiu College of Technology, Kaohsiung, Taiwan 80741, R.O.C., and
[2] Department of Chemical Engineering, National Cheng-Kung University, Tainan, Taiwan 70101, R.O.C.

SYNOPSIS

A series of new alkene and octenyloxy monomers containing 4′-[oligo(ethylene oxide)]*n* monomethyl ether 4-biphenyl ether carboxyl benzoate [MS3BDBE$_n$] (n = 1 to 3) and 1-(*p*-methoxydiphenyl)-(carboxyl benzoate) [oligo(ethylene oxide)]*n* [MS$_{m+2}$BE*n*DB] (m = 1, 6; n = 1 to 3) as end groups were synthesized. The molecular structure of the monomers was characterized using nuclear magnetic resonance (NMR) spectroscopy. These monomers were grafted onto poly(methylhydrosiloxane)s (PMHS) by the platinum-catalyzed hydrosilylation process. The thermal transition temperatures and mesophase textures of the monomers and the polysiloxane polymers have been determined by differential scanning calorimetry (DSC) and by polarized optical microscopy. The effect of changes in chemical structure on the mesophase properties, glass transition temperature, isotropic temperature, and mesophase texture of the monomers and the polysiloxane polymers is discussed. Polymers PS3BDBE*n* showed smectic and nematic phases which were not analogous to their precursor nematic monomers MS3BDBE*n*. Both monomers MS$_{m+2}$BE$_n$DB and their polymeric homologous PS$_{m+2}$BE$_n$DB did not exhibit mesophase properties. This demonstrated that the polymer effect could not stabilize the mesophase obtained from mesogenic core which contained a flexible oligo(ethylene oxide) unit interconnecting aromatic group. © 1995 John Wiley & Sons, Inc.

INTRODUCTION

The potential uses of side-chain liquid crystalline polymers (SCLCPs) have received much attention recently.[1-4] Because of their particular properties, thermotropic side-chain LC polymers have been examined as potential advanced materials for speciality applications, such as information storage media,[5-7] elements requiring nonlinear optical characteristics,[8-9] piezo-, pyro-, and ferroelectric devices,[10] and the stationary phase in columns for high-efficiency gas chromatography.[11,12] Synthesis, structure–property relations, and application were concisely reviewed by Varshney[13] and Gray et al.[14]

We recently reported on the synthesis and thermotropic properties of a series of polysiloxane backbone polymers. The side-chain molecules (I, II, and III) were terminated with an oligo(ethylene oxide)monomethyl ether group of variable length connected via an ester linkage with mesogenic core (with a variable length methylene spacer).

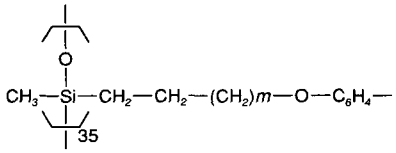

$$\text{COO}-\text{C}_6\text{H}_4-\text{C}_6\text{H}_4-\text{COO}-(\text{C}_2\text{H}_4\text{O})n-\text{CH}_3 \quad \text{(I)}$$

m = 1, 3, 8; n = 1, 2, 3

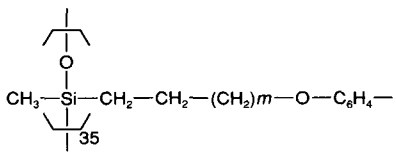

$$\text{C}_6\text{H}_4-\text{COO}-\text{C}_6\text{H}_4-\text{COO}-(\text{C}_2\text{H}_4\text{O})n-\text{CH}_3 \quad \text{(II)}$$

m = 1; n = 2

* To whom correspondence should be addressed.

Journal of Applied Polymer Science, Vol. 57, 1183–1204 (1995)
 CCC 0021-8995/95/101183-22

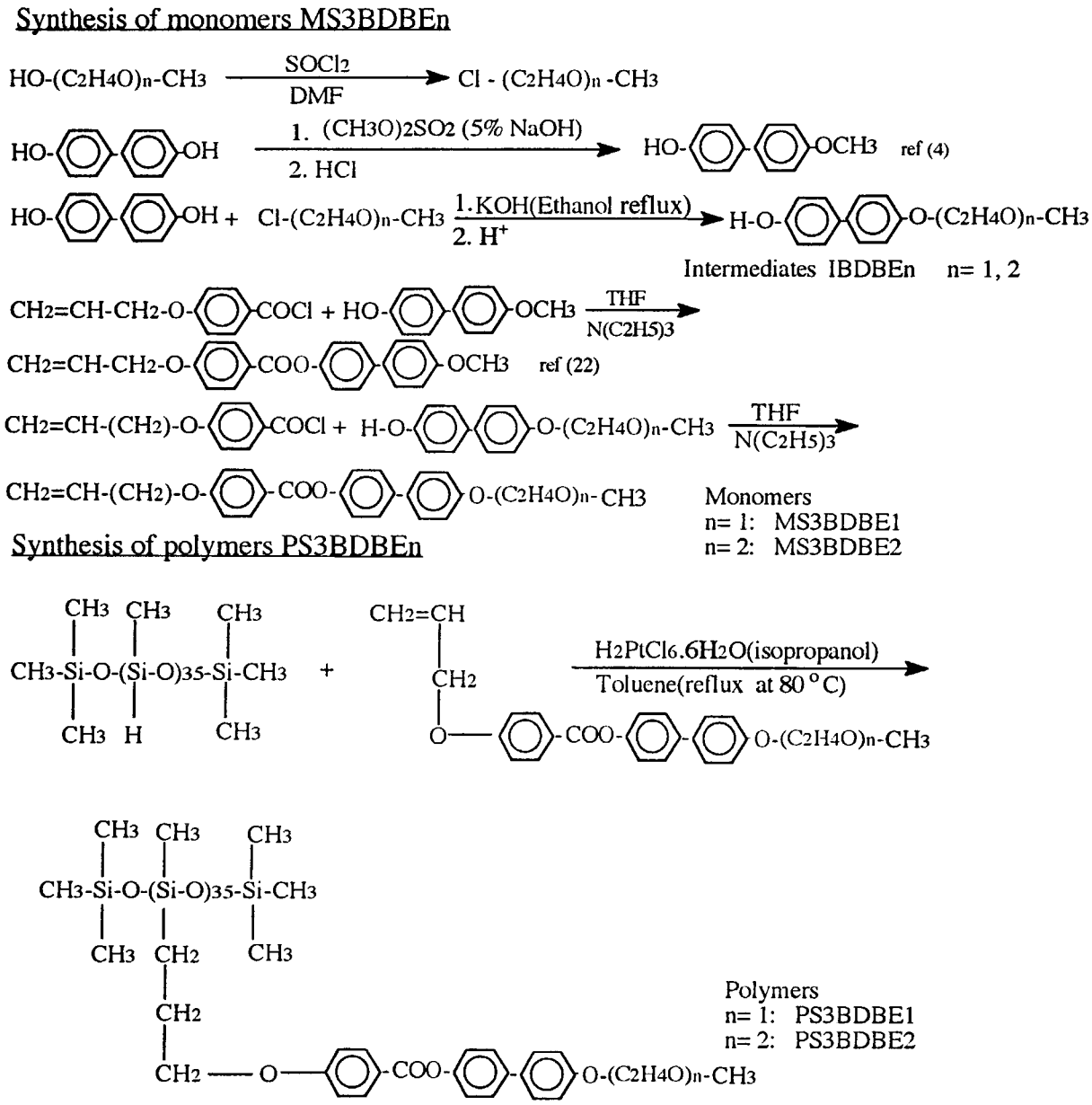

Scheme 1 Preparation of the monomer MS3BDBE*n* and the polysiloxane polymer PS3BDBE*n*.

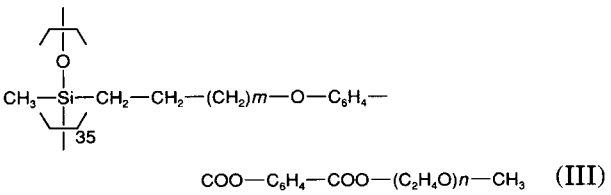

COO—C_6H_4—COO—$(C_2H_4O)n$—CH_3 (III)

m = 1; *n* = 0, 1, 2

Polymers I and II showed a smectic C liquid crystalline mesophase.[15-17] The length of the terminal group profoundly influenced the thermal transition temperatures and mesophase texture. In contrast to the carboxyl alkyl terminal group,[18] polymer III did not show mesomorphic properties. For the carboxyl oligo(ethylene oxide)monomethyl ether terminal group, the instability of the mesogenic unit might be caused by the motion of the flexible terminal group. The constraits, generated by the polymer chains, cannot overcome the motion.

The concept of replacing interconnecting ester groups of mesogenic units with flexible groups

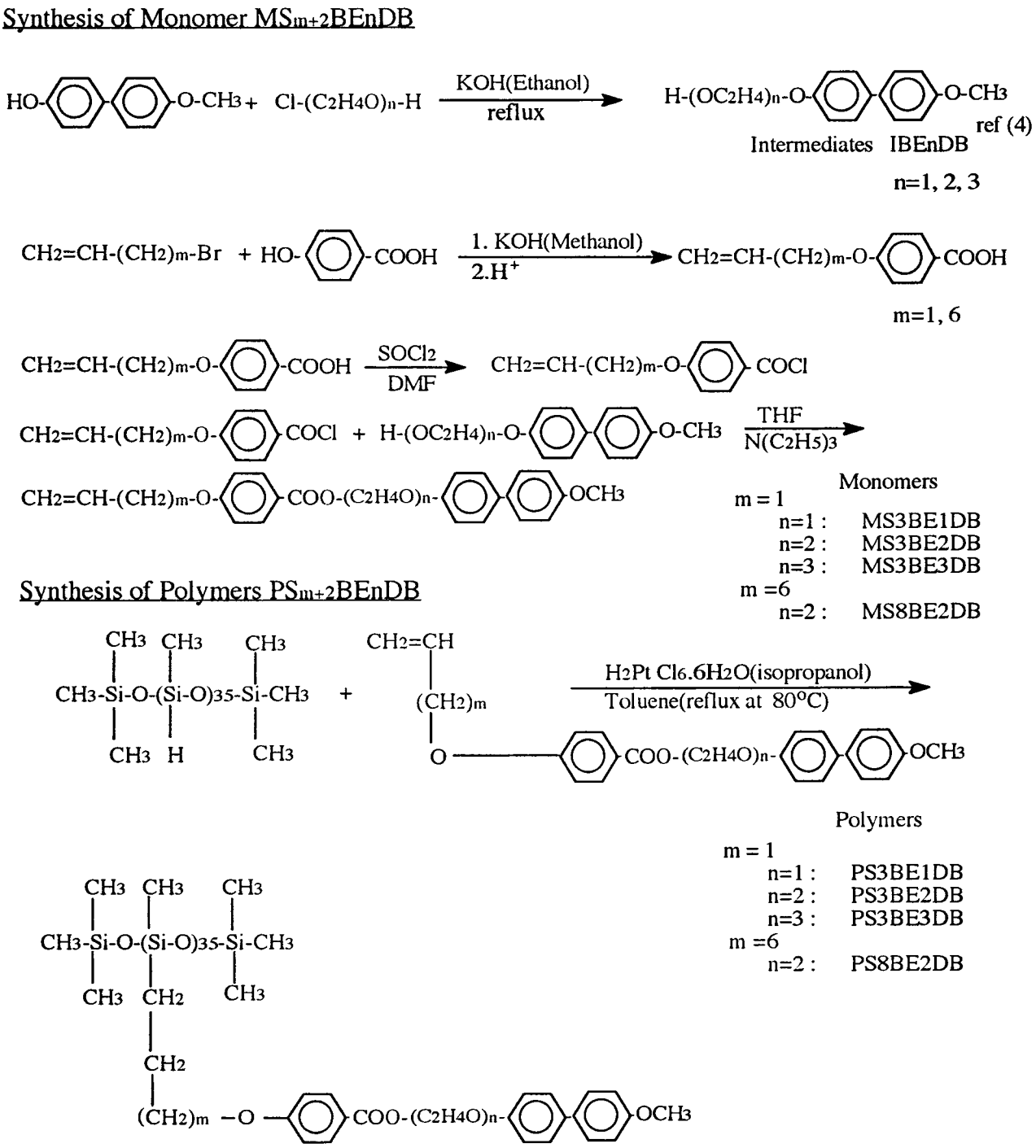

Scheme 2 Preparation of the monomers MS*m*+2BE*n*DB and the polysiloxane polymers PS*m*+2BE*n*DB.

(e.g., methyleneoxy or ethane) has recently received attention by organic chemists working in the field of low molar mass liquid crystalline. Most of the low molar mass liquid crystals based on benzyl ethers present only monotropic or virtual transition,[19,20] and their corresponding polymers exhibit enantiotropic mesomorphism. To understand how the flexible oligo(ethylene oxide) linkages affect the thermal properties and enantiotropic mesomorphism of the monomers and polymers, a number of polysiloxane polymers with the following side chain were synthesized:

Table I ^{1}H-NMR Chemical Shifts for the Monomers in This Study

Monomers	200 MHz ^{1}H-NMR ($CDCl_3$, δ ppm)
MS3BDBE0	3.86(s, —OC$\underline{H}_3$); 4.64(m, —C$\underline{H}_2$O—Ph—); 5.44 ~ 5.46(m, C$\underline{H}_2$=CH—); 6.06 ~ 6.12(m, CH_2=C$\underline{H}$—); 6.98 ~ 7.02(m, 2H aromatic protons); 7.25 ~ 7.27(m, 2H aromatic protons); 7.52 ~ 7.60(m, 4H aromatic protons); 8.16 ~ 8.19(m, 4H 7.03 ~ 8.19 aromatic protons)
MS3BDBE1	3.47(s, —OC$\underline{H}_3$); 3.77 ~ 3.79(m, —C$\underline{H}_2$OCH$_3$); 4.17 ~ 4.18(m, —Ph—Ph—O—C$\underline{H}_2$—); 4.63 ~ 4.65(m, CH_2=CHC$\underline{H}_2$—O—Ph—); 5.33 ~ 5.49(m, C$\underline{H}_2$=CH—); 6.04 ~ 6.11(m, CH_2=C$\underline{H}$—); 6.99 ~ 7.02(m, 4H aromatic protons); 7.23 ~ 7.26(m, 2H aromatic protons); 7.50 ~ 7.59(m, 4H aromatic protons); 8.16 ~ 8.19(m, 2H aromatic protons)
MS3BDBE2	3.39(s, —OC$\underline{H}_3$); 3.62 ~ 3.74(m, —C$\underline{H}_2$—O—CH_3); 3.71 ~ 3.77(m, —Ph—OCH$_2$C$\underline{H}_2$—); 3.83 ~ 3.93(m, —O—C$\underline{H}_2$—CH_2—O—C$\underline{H}_2$—CH_2—O—CH_3); 4.17 ~ 4.23(m, —Ph—Ph—O—CH_2—C$\underline{H}_2$—O—); 4.62 ~ 4.66(m, CH_2=CH—C$\underline{H}_2$—O—Ph); 5.33 ~ 5.47(m, C$\underline{H}_2$=CH—); 6.01 ~ 6.12(m, CH_2=C$\underline{H}$—); 6.98 ~ 7.02(m, 4H aromatic protons); 7.25 ~ 7.27(m, 2H aromatic protons); 7.52 ~ 7.60(m, 4H aromatic protons); 8.16 ~ 8.19(m, 2H aromatic protons)
MS3BE1DB	3.84(s, —OC$\underline{H}_3$); 4.32 ~ 4.35(m, —COO—CH_2—C$\underline{H}_2$—O—Ph—Ph—); 4.57 ~ 4.59(m, CH_2=CH—C$\underline{H}_2$—O—Ph—); 4.64 ~ 4.67(m, —Ph—COO—C$\underline{H}_2$—CH_2); 5.44 ~ 5.46(m, C$\underline{H}_2$=CH—); 6.06 ~6.12(m, CH_2=C$\underline{H}$—); 6.91 ~ 6.929(m, 2H aromatic protons); 6.934 ~ 7.012(m, 2H aromatic protons); 7.25 ~ 7.49(m, 4H aromatic protons); 7.99 ~ 8.01(m, 4H 7.03 ~ 8.19 aromatic protons)
MS3BE2DB	3.84(s, —OC$\underline{H}_3$); 3.91 ~ 3.94(m, —COO—CH_2—C$\underline{H}_2$—O—C$\underline{H}_2$—CH_2—O—Ph—Ph—); 4.17 ~ 4.20(m, —C$\underline{H}_2$—O—Ph—Ph—); 4.48 ~ 4.50(m, —O—Ph—COO—C$\underline{H}_2$—CH_2—); 4.54 ~ 4.56(m, CH_2=CH—C$\underline{H}_2$—O—Ph—); 5.32 ~ 5.43(m, C$\underline{H}_2$=CH—); 6.06 ~ 6.10(m, CH_2=C$\underline{H}$—); 6.89 ~ 6.91(m, 2H aromatic protons; 6.95 ~ 6.99(m, 4H aromatic protons); 7.45 ~ 7.49(m, 4H aromatic protons); 7.995 ~ 8.01(m, 2H 7.03 ~ 8.19 aromatic protons)
MS3BE3DB	3.84(s, —OC$\underline{H}_3$); 3.75 ~ 3.89(m, —COO—CH_2—(C$\underline{H}_2$O)4—CH_2—O—Ph—Ph—); 4.14 ~ 4.15(m, —C$\underline{H}_2$—O—O—Ph—Ph—); 4.57 ~4.59(m, —Ph—COO—C$\underline{H}_2$—CH_2—); 4.63 ~ 4.67(m, CH_2=CH—C$\underline{H}_2$—O—Ph—); 5.29 ~ 5.43(m, C$\underline{H}_2$=CH—); 5.99 ~ 6.06(m, CH_2=C$\underline{H}$—); 6.90 ~ 6.92(m, 2H aromatic protons); 6.93 ~ 6.97(m, 4H aromatic protons); 7.27 ~ 7.48(m, 4H aromatic protons); 8.01 ~ 8.02(m, 2H 7.03 ~ 8.19 aromatic protons)
MS8BE2DB	1.39 ~ 2.09(3m, CH_2=CH—(C$\underline{H}_2$)$_5$—); 3.84(s, —OC$\underline{H}_3$); 3.91 ~ 3.98(m, —COO—CH_2—C$\underline{H}_2$—O—C$\underline{H}_2$—CH_2—O—Ph—Ph—and—C$\underline{H}_2$—O—Ph—); 4.17 ~ 4.19(m, —C$\underline{H}_2$—O—Ph—Ph—); 4.48 ~ 4.51(m, —Ph—COO—C$\underline{H}_2$—CH_2—); 5.44 ~ 5.46(m, C$\underline{H}_2$=CH—); 6.06 ~ 6.12(m, CH_2=C$\underline{H}$—); 6.87 ~ 6.89(m, 2H aromatic protons); 6.95 ~ 6.99(m, 4H aromatic protons); 7.45 ~ 7.49(m, 4H aromatic protons); 7.99 ~ 8.02(m, 2H 7.03 ~ 8.19 aromatic protons)

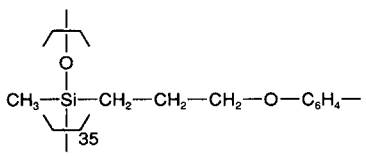

COO—C_6H_4—C_6H_4—O—(C_2H_4O)n—CH_3 (IV)

n = 1 to 3

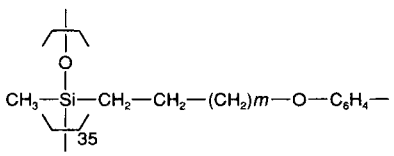

COO—(C_2H_4O)n—C_6H_4—C_6H_4—O—CH_3 (V)

n = 1 to 3; m = 1, 8

Table II Carbon Chemical Shifts for the Monomers in This Study

MS3BDBE0

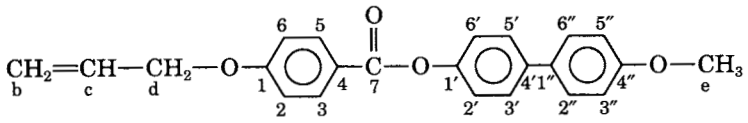

C_b = 118.21	C_c = 132.45	C_d = 68.93	C_e = 55.33			
C_1 = 162.90	C_2 = 114.55	C_3 = 132.28	C_4 = 121.99	C_5 = 132.28	C_6 = 114.55	C_7 = 164.93
$C_{1'}$ = 150.02	$C_{2'}$ = 127.69	$C_{3'}$ = 121.97	$C_{4'}$ = 133.03	$C_{5'}$ = 121.97	$C_{6'}$ = 127.69	
$C_{1''}$ = 138.42	$C_{2''}$ = 114.24	$C_{3''}$ = 128.13	$C_{4''}$ = 159.17	$C_{5''}$ = 128.13	$C_{6''}$ = 114.24	

MS3BDBE1

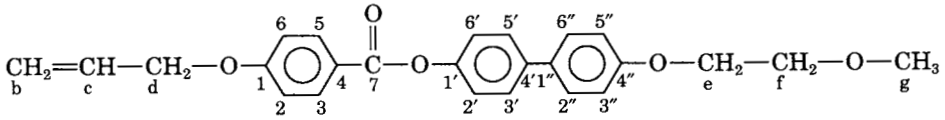

C_b = 118.19	C_c = 132.45	C_d = 68.92	C_e = 67.37	C_f = 71.04	C_g = 59.20	
C_1 = 162.89	C_2 = 114.94	C_3 = 132.26	C_4 = 121.97	C_5 = 132.26	C_6 = 114.94	C_7 = 164.93
$C_{1'}$ = 150.03	$C_{2'}$ = 127.68	$C_{3'}$ = 121.95	$C_{4'}$ = 133.24	$C_{5'}$ = 121.95	$C_{6'}$ = 127.68	
$C_{1''}$ = 138.44	$C_{2''}$ = 114.54	$C_{3''}$ = 128.09	$C_{4''}$ = 158.37	$C_{5''}$ = 128.09	$C_{6''}$ = 114.54	

MS3BDBE2

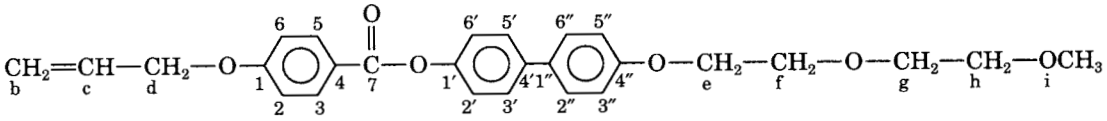

C_b = 118.21	C_c = 132.44	C_d = 68.89	C_e = 67.36	C_f = 71.03	C_g = 71.67	C_h = 71.49	
C_i = 59.20							
C_1 = 162.88	C_2 = 114.34	C_3 = 132.24	C_4 = 121.98	C_5 = 132.24	C_6 = 114.34	C_7 = 164.94	
$C_{1'}$ = 150.04	$C_{2'}$ = 127.67	$C_{3'}$ = 121.93	$C_{4'}$ = 150.01	$C_{5'}$ = 121.93	$C_{6'}$ = 127.67		
$C_{1''}$ = 138.43	$C_{2''}$ = 114.55	$C_{3''}$ = 128.11	$C_{4''}$ = 158.35	$C_{5''}$ = 128.11	$C_{6''}$ = 114.55		

MS3BE1DB

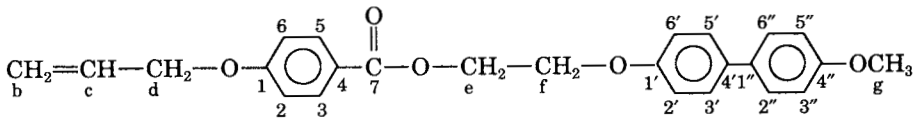

C_b = 118.10	C_c = 132.52	C_d = 68.84	C_e = 63.11	C_f = 66.27	C_g = 55.3	
C_1 = 162.48	C_2 = 114.17	C_3 = 131.76	C_4 = 122.42	C_5 = 131.76	C_6 = 114.17	C_7 = 166.22
$C_{1'}$ = 157.74	$C_{2'}$ = 127.73	$C_{3'}$ = 114.91	$C_{4'}$ = 133.36	$C_{5'}$ = 114.91	$C_{6'}$ = 127.73	
$C_{1''}$ = 133.98	$C_{2''}$ = 114.32	$C_{3''}$ = 127.77	$C_{4''}$ = 158.76	$C_{5''}$ = 127.77	$C_{6''}$ = 114.32	

MS3BE2DB

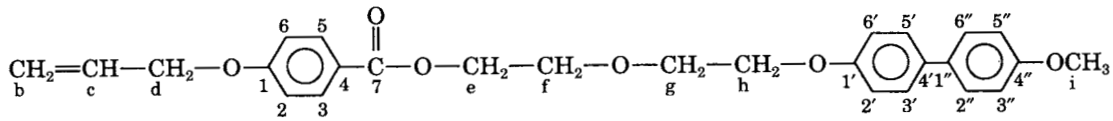

C_b = 117.98	C_c = 132.51	C_d = 68.74	C_e = 63.77	C_f = 69.70	C_g = 69.46	C_h = 67.54	C_i = 55.26
C_1 = 162.33	C_2 = 114.12	C_3 = 131.64	C_4 = 122.55	C_5 = 131.64	C_6 = 114.12	C_7 = 166.19	
$C_{1'}$ = 157.81	$C_{2'}$ = 127.59	$C_{3'}$ = 114.89	$C_{4'}$ = 133.32	$C_{5'}$ = 114.89	$C_{6'}$ = 127.59		
$C_{1''}$ = 133.59	$C_{2''}$ = 114.24	$C_{3''}$ = 127.61	$C_{4''}$ = 158.66	$C_{5''}$ = 127.61	$C_{6''}$ = 114.24		

Table II *Continued*

MS3BE3DB

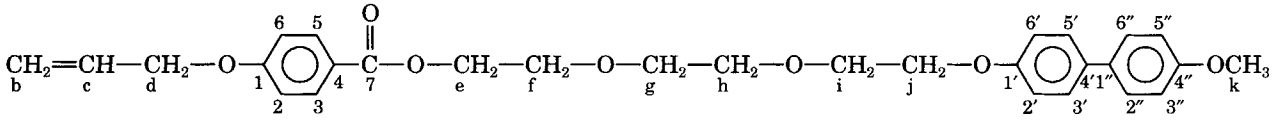

C_b = 117.98	C_c = 132.49	C_d = 68.74	C_e = 63.76	C_f = 69.70	C_g = 70.77	C_h = 70.70	C_i = 69.30
C_j = 67.47	C_c = 55.26						
C_1 = 162.33	C_2 = 114.23	C_3 = 131.63	C_4 = 122.60	C_5 = 131.63	C_6 = 114.23	C_7 = 166.17	
$C_{1'}$ = 157.84	$C_{2'}$ = 127.57	$C_{3'}$ = 114.84	$C_{4'}$ = 133.33	$C_{5'}$ = 114.84	$C_{6'}$ = 127.57		
$C_{1''}$ = 133.55	$C_{2''}$ = 114.10	$C_{3''}$ = 127.61	$C_{4''}$ = 158.65	$C_{5''}$ = 127.61	$C_{6''}$ = 114.10		

MS8BE2DB

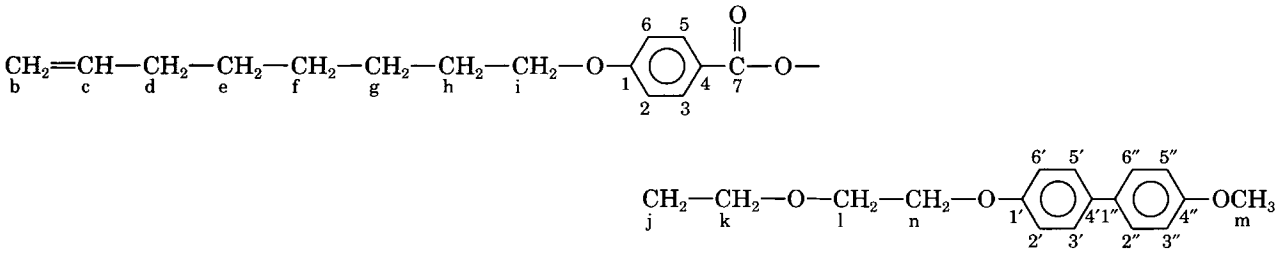

C_b = 114.26	C_c = 138.84	C_d = 33.58	C_e = 28.66	C_f = 28.69	C_g = 25.73	C_h = 28.96	C_i = 68.02
C_j = 63.70	C_k = 69.66	C_l = 69.44	C_m = 67.51	C_n = 55.21			
C_1 = 162.92	C_2 = 114.08	C_3 = 131.61	C_4 = 122.15	C_5 = 131.61	C_6 = 114.08	C_7 = 166.23	
$C_{1'}$ = 157.80	$C_{2'}$ = 127.32	$C_{3'}$ = 114.87	$C_{4'}$ = 133.29	$C_{5'}$ = 114.87	$C_{6'}$ = 127.32		
$C_{1''}$ = 133.55	$C_{2''}$ = 113.96	$C_{3''}$ = 127.56	$C_{4''}$ = 158.64	$C_{5''}$ = 127.56	$C_{6''}$ = 113.96		

Polymers IV has an "ether" linkage mesogenic core and a terminal ether oligo(ethylene oxide)monomethyl ether group. Polymers V had an oligo(ethylene oxide) unit inserted between the carboxyl benzoate and biphenyl group. The goal of this study was to present the synthesis and characterization of a series of liquid crystalline polysiloxane polymers (IV) and (V), to compare the thermal properties with different chain linkages, and to study the role of the interconnecting group between the aromatic groups.

EXPERIMENTAL

Materials

p-Hydroxybenzoic acid, 2-chloroethanol, 2-(2-chloroethoxy)ethanol, 2-[2-(2-chloroethoxy)ethoxy]ethanol, 2-methoxy ethanol, diethylene glycol monomethyl ether, triethylene glycol monomethyl ether, allyl bromide (from Tokyo Chemical Industry Co., Ltd.) were used as received. 4,4′-Dihydroxy biphenyl, polymethylhydrosiloxanes [with $\overline{DP}$ = 35, $\overline{Mw} \approx 2300$], and hexachloroplatinic acid (from E. Merck Co.) were used as received. 8-Bromo-1-octene (from Fluka Chemika-BioChemika Co., Ltd.) was used as received. Toluene, used in the hydrosilylation reaction, was first refluxed over sodium and then distilled under nitrogen.

Techniques

^{1}H-NMR spectra and two-dimensional NMR spectra were respectively recorded on a Bruker AC200 (200.13 MHz) and a Bruker AC400 (400.13 MHz) from a $CDCl_3$ solution with TMS as internal standard. The phase transition temperatures of the monomers and the polymers were studied using a Perkin–Elmer DSC-7 differential scanning calo-

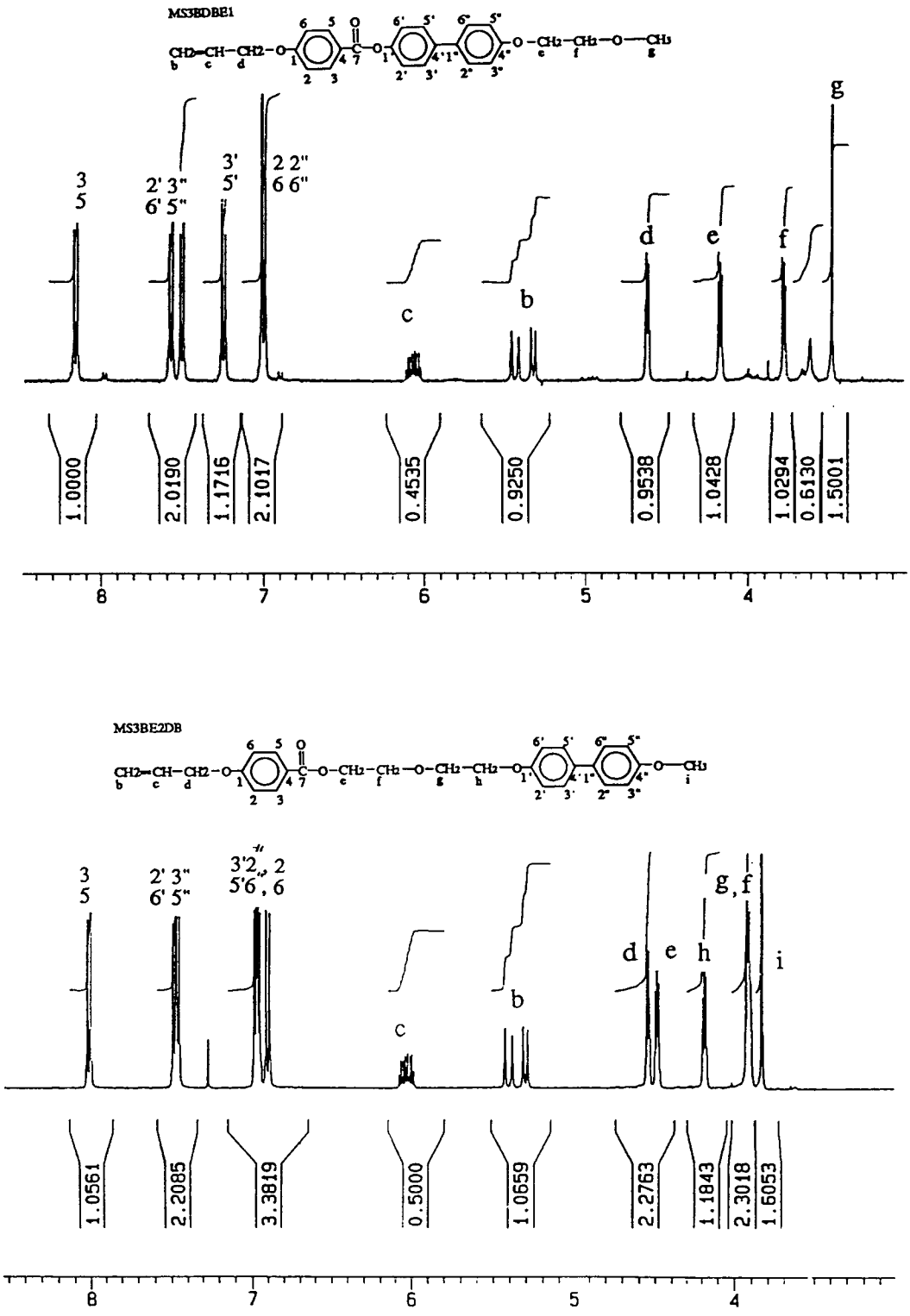

Figure 1 200-MHz ^{1}H-NMR spectra of monomers MS3BDBE1 and MS3BE2DB.

rimeter with a central processor and an interior cooler II for the cooling experiment. The anisotropic textures of the monomers and polymers were observed with an Olympus BH-2 polarized optical microscope with a Linkam THMS 600 hot stage and a TMS 91 central temperature control processor.

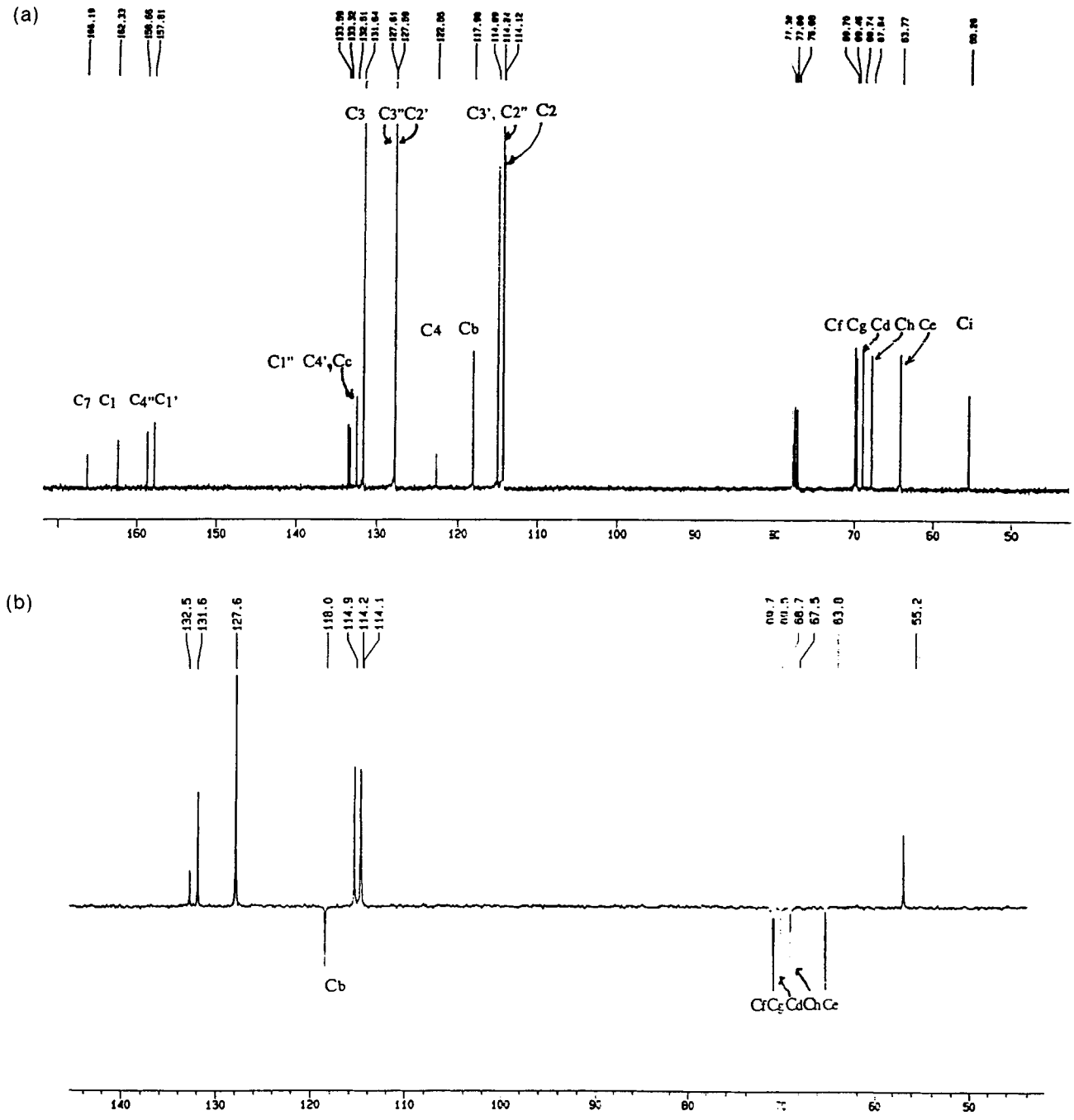

Figure 2 400-MHz two-dimensional NMR spectra of monomer MS3BE2DB. (a) ^{13}C-NMR spectrum, (b) DEPT 135 spectrum, (c) HMBC spectrum, (d) HMBC spectrum, (e) HMQC spectrum, (f) COSY 90 spectrum.

Synthesis

Synthesis of Monomers ME1S3 and ME2S3

These were synthesized as reported in a previous publication from our laboratory.[15] Synthesis of monomers MS3BDBE*n* and MS*m*+2BE*n*DB and polymers PS3BDBE*n* and PS*m*+2BE*n*DB are outlined in Schemes 1 and 2, respectively.

Synthesis of Monomer MS3BDBEn (n = 0, 1, 2)

Synthesis of 2-Chloroethylene Methyl Ether and 2-(2-Chloroethoxy)Ethylene Methyl Ether. 2-Chlo-

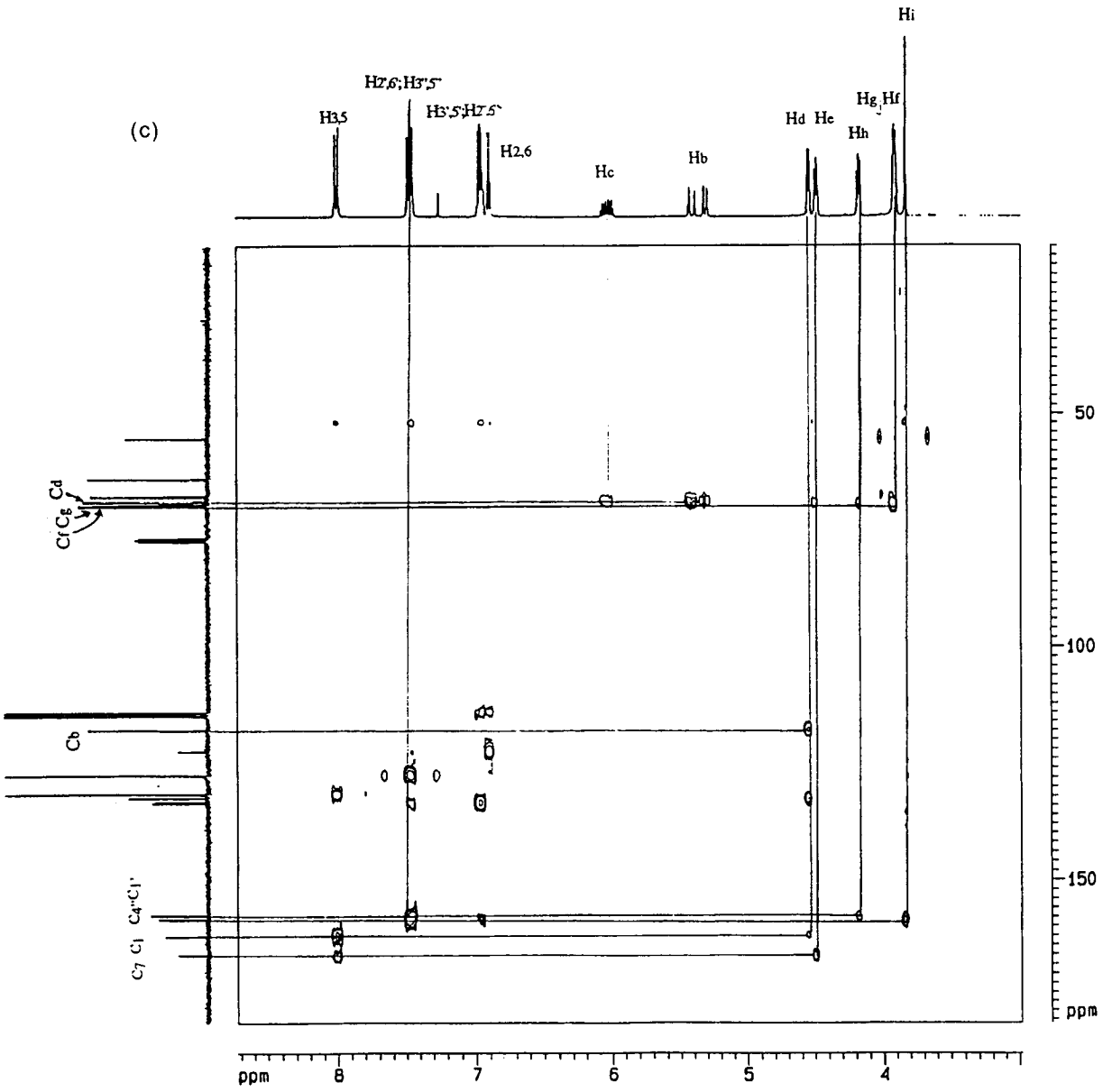

Figure 2. (*Continued from the previous page*)

roethylene methyl ether and 2-(2-chloroethoxy) ethylene methyl ether were respectively synthesized from 2-methoxy ethanol and diethylene glycol monomethyl ether by the chloride substitution reaction. The example of 2-chloroethylene methyl ether is as follows: 2-Methoxy ethanol, 20 g (0.263 mol), was placed in a 250-mL two-neck round flask, equipped with an addition funnel and an absorption HCl apparatus. Thionyl chloride (60 mL) was added slowly, followed by 5 drops of dimethylforamide (DMF). The reaction mixture was then refluxed at 70°C for 5 h. After reaction completion, the dark brown solution was stirred into 200 mL distilled water. This solution was extracted twice with 100 mL dichloromethane. The organic layer was washed with saturated sodium bicarbonate solution twice, with water twice, and then dried over anhydrous magnesium sulfate ($MgSO_4$). The solution was removed with a rotary evaporator under reduced pressure. The residual solution was further purified by vacuum distillation. Finally, 21 g of 2-chloroethylene methyl ether was obtained (yield 84.5%). The characteristic absorption peak of the OH group at 3450 cm^{-1} was

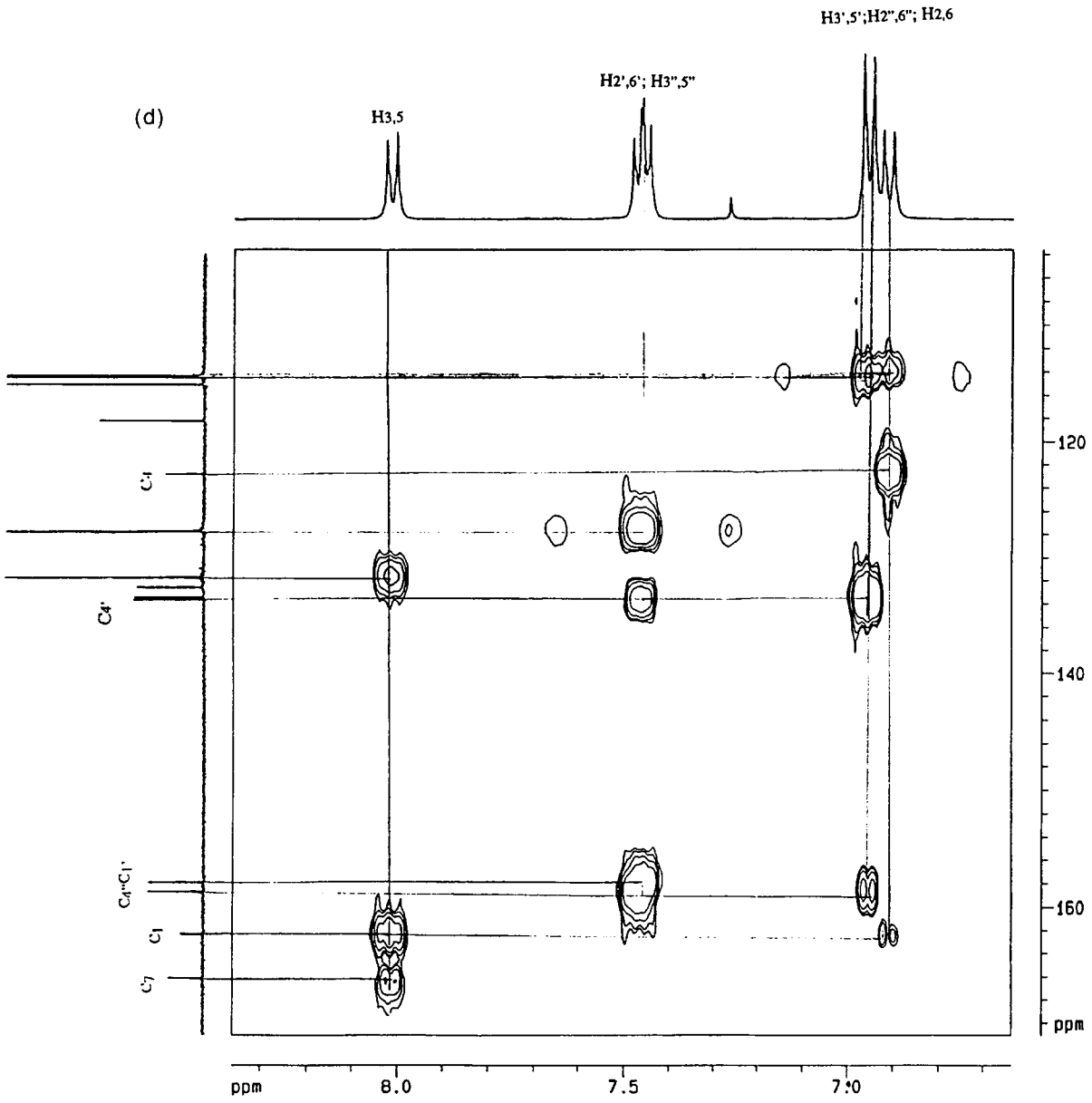

Figure 2. (*Continued from the previous page*)

not observed, indicating that the OH group was completely substituted by chloride. 2-(2-Chloroethoxy)ethylene methyl ether (an 80% yield) was obtained consistently.

Synthesis of Intermediate Compounds IBDBE0, IBDBE1, and IBDBE2. 4-Methoxy-4'-hydroxybiphenyl (IBDBE0) was synthesized according to the procedure of Percec et al.[4] [melting point (mp) 178 to 181°C (ref. 4) mp 179 to 181°C]. The intermediate compounds IBDBE1 and IBDBE2 were synthesized by the same methods. An example of IBDBE2 is presented: 4,4'-dihydroxy biphenyl (10 g, 0.054 mol) and NaOH (4.32 g, 1.08 mol) were placed in a 500-mL round flask reactor which contained 120 mL ethanol solution. The mixture solution was refluxed until the 4,4'-dihydroxy biphenyl became the sodium salt (approximately 0.5 h). 2-(2-Chloroethoxy)ethylene methyl ether (8.23 g, 0.059 mol) was added to the aforementioned brown solution and was refluxed overnight (the mixture solution became light yellow). The solution was poured into water and acidified by 6 *M* HCl. The precipitated product was filtered, washed with 5% NaOH solution, followed by water,

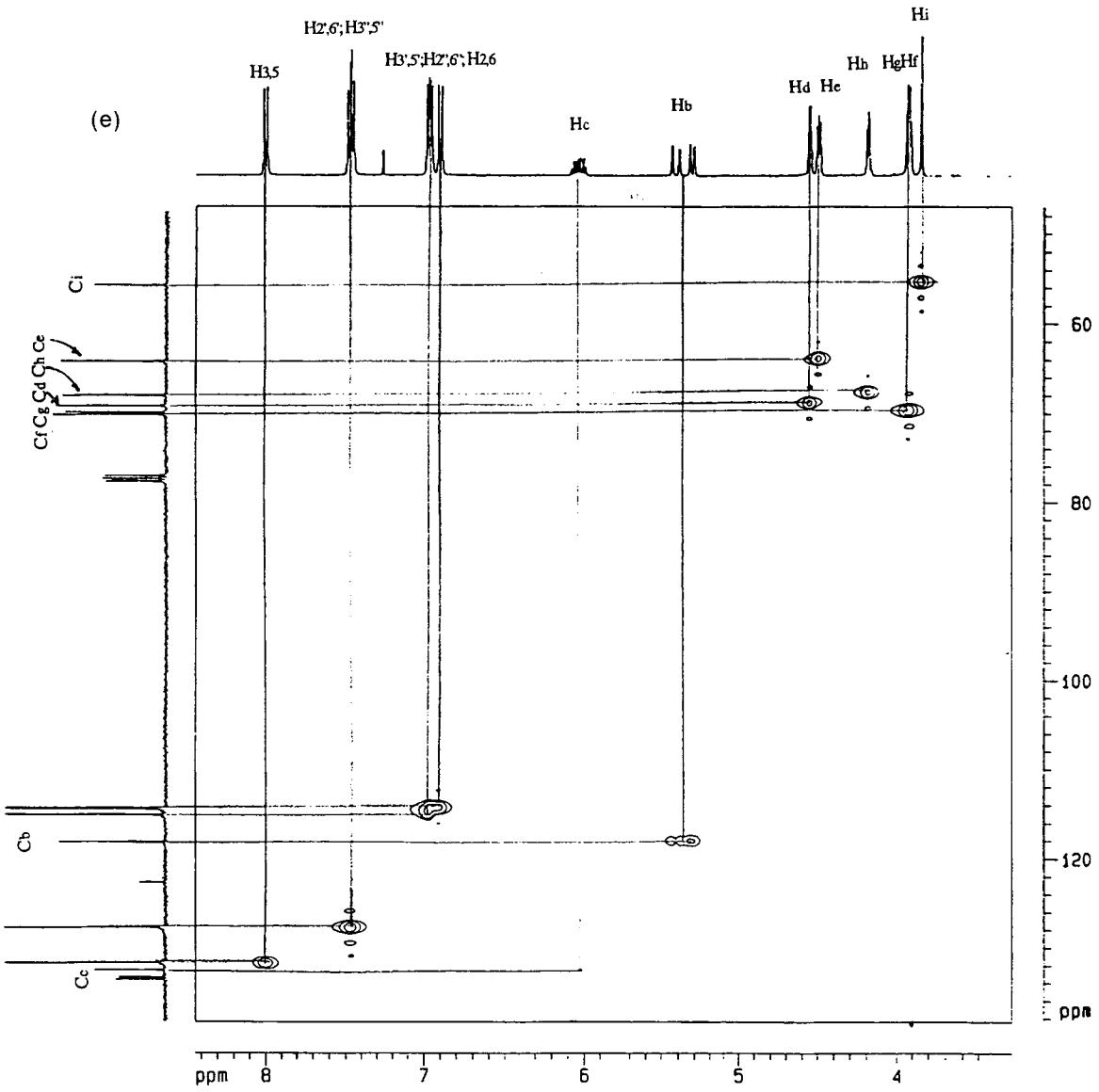

Figure 2. (*Continued from the previous page*)

and dried in vacuum oven at 45°C. The crude product was further purified in a silica gel packed column, with CH_2Cl_2/*n*-hexane/methanol (20 v/5 v/1 v) as the mobile phase to obtain 7.0 g of pure product (yield 45%; mp = 153°C). IBDBE1 : CH_2Cl_2/*n*-hexane/methanol (40 v/5 v/1 v) was the mobile phase (yield 52%; mp = 109°C).

Synthesis of Monomers MS3BDBE0, MS3BDBE1, and MS3BDBE2. Monomer MS3BDBE0 was synthesized according to the procedure of Apfel et al.[22] Both monomers MS3BDBE1 and MS3BDBE2 were synthesized by the same procedure. An example of MS3BDBE2 follows: 0.0267 mol 4-allyloxy benzoic acid (4.753 g) and 16 mL thionyl chloride containing a drop of DMF were reacted until the solution became clear (approximately 3 h). The excess thionyl chloride was removed by a vacuum rotary evaporator to obtain yellow, viscous 4-allyloxybenzoyl chloride. The acid chloride was dissolved in 5 mL CH_2Cl_2 and slowly added to a solution of 0.0243 mol 7.0 g) intermediate compound IBDBE2 with an excess mole ratio of dry triethylamine in 50 mL of CH_2Cl_2 in an ice water bath to incur a reaction. CH_2Cl_2 and triethylamine in the reaction solution were removed by the rotary evaporator under reduced pressure. The residual material was purified in a silica gel packed column with CH_2Cl_2/*n*-hexane/methanol (20 v/5 v/1 v) as the mobile

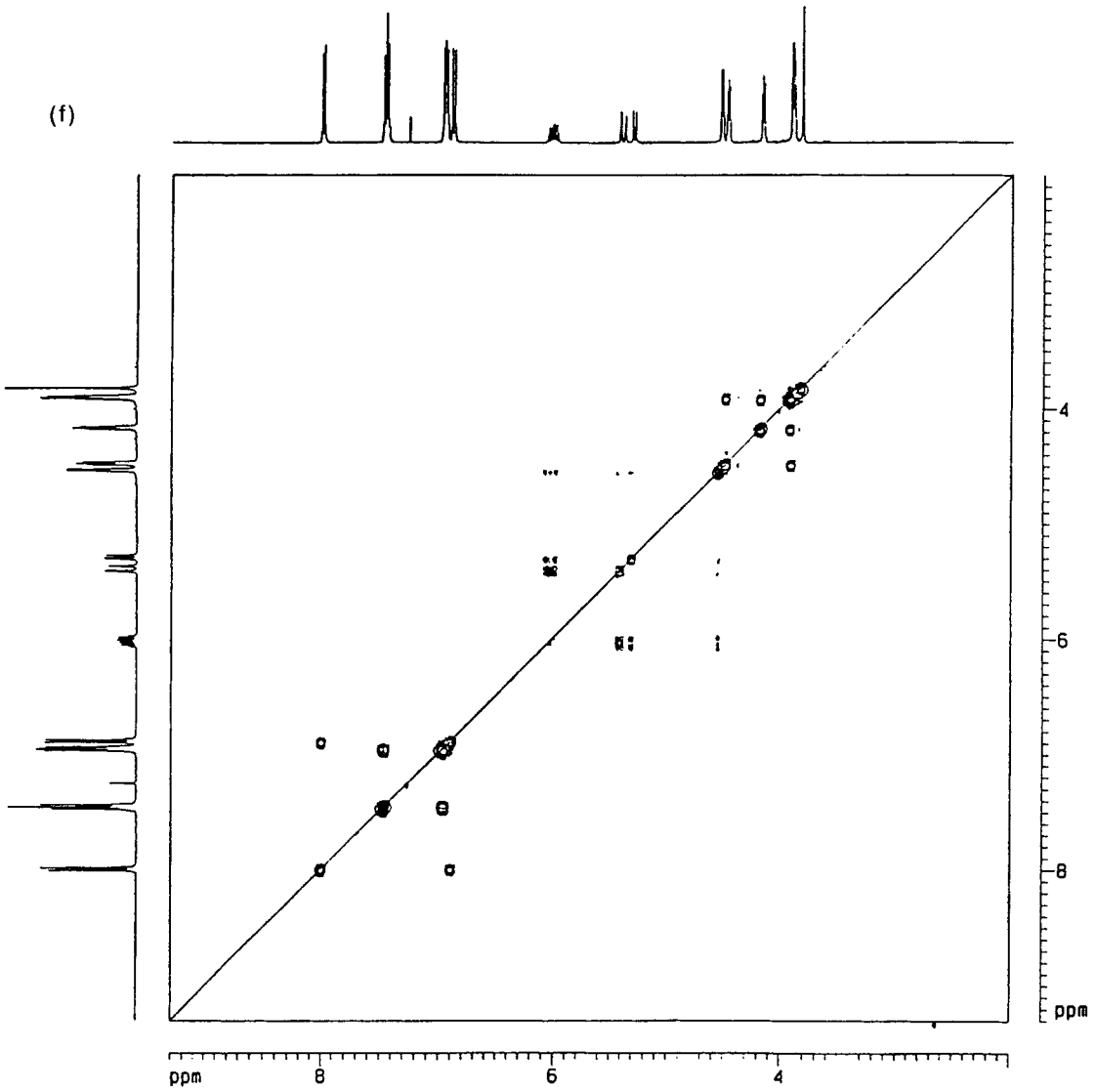

Figure 2. (*Continued from the previous page*)

phase to obtain a pure product, 6.35 g (yield 60%); MS3BDBE1 : CH_2Cl_2/*n*-hexane/methanol (40 v/10 v/1 v) was the mobile phase (yield 65%). The characteristic ^{1}H-NMR and ^{13}C-NMR chemical shifts of the monomer MS3BDBE*n* are respectively summarized in Tables I and II.

Synthesis of Monomers MSm+2Ben**DB (m = 1,6; n = 1,2,3)**

Synthesis of Intermediate Compounds IBE1DB, IBE2DB, and IBE3DB. All the intermediates IBE1DB, IBE2DB, and IBE3DB were synthesized after a modification of the procedure of Percec et al.[4] An example of IBE2DB is presented. 4-Methoxy-4′-hydroxy biphenyl (10 g, 0.05 mol) and KOH (3.4 g, 0.06 mol) were dissolved in 200 mL of ethanol solution (80% volume ratio ethanol). 2-(2-Chloroethoxy) ethanol (7.5 g, 0.06 mol) was added and the solution was refluxed overnight. The reaction mixture was then poured into water. The precipitated product was filtered, washed with 5% NaOH solution followed by water, and dried under vacuum at 45°C. The crude product was further purified in a silica gel packed column with CH_2Cl_2/*n*-hexane/methanol (40 v/10 v/2 v) as the mobile phase to obtain 9.2 g of pure product (yield 64%; mp = 123°C); IBE1DB : CH_2Cl_2/*n*-hexane/methanol (40 v/10 v/1 v) was the mobile phase (yield 70%; mp = 171°C); IBE3DB : CH_2Cl_2/*n*-hexane/meth-

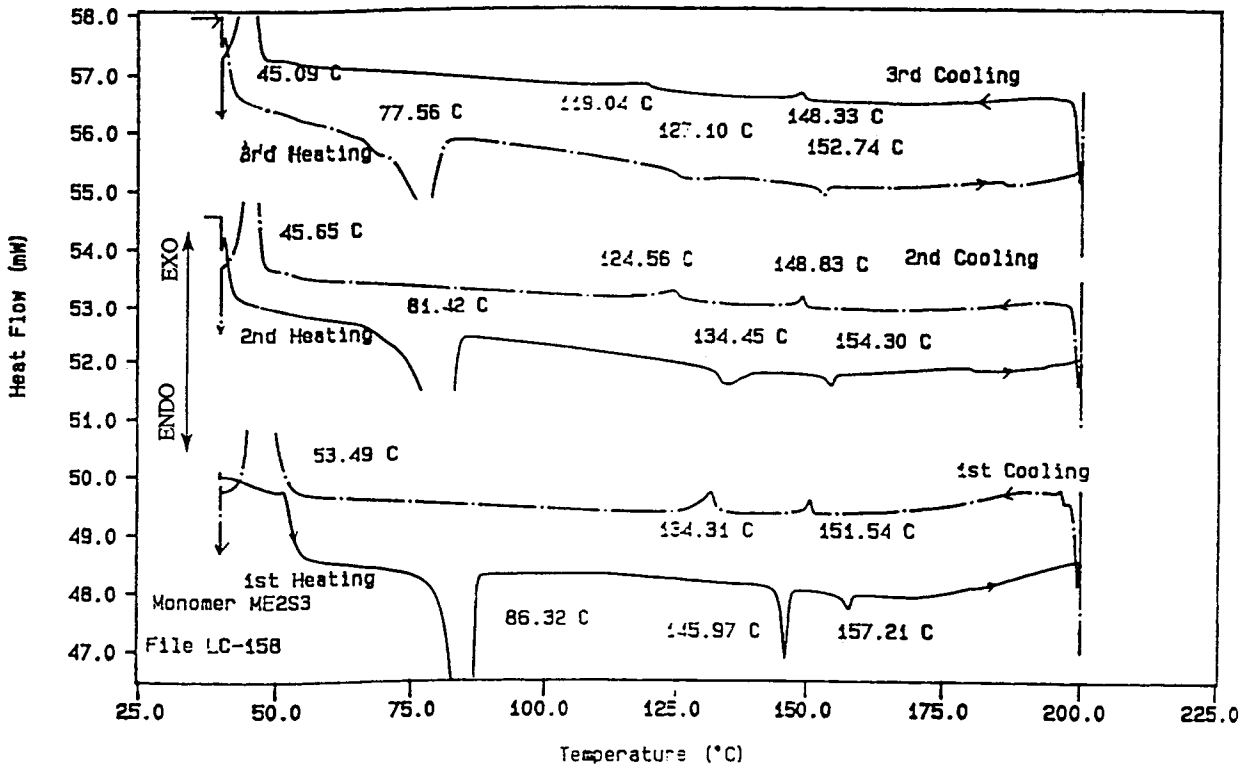

Figure 3 DSC thermograms of the monomer ME2S3 in a repeated heating and cooling experiment (heating and cooling rate of 10°C/min).

anol (40 v/10 v/3 v) was the mobile phase (yield 65%; mp = 96°C).

Synthesis of monomer MSm+2BEnDB (m = 1,6; n = 1,2,3)

All the monomers were synthesized by esterification of the corresponding intermediate compounds IBE*n*DB (n = 1 to 3) with allyloxy benzoyl chloride and 4-octenyloxy benzoyl chloride. An example of MS3BE2DB follows: 0.021 mol 4-allyloxy benzoic acid (3.738 g) and 12 mL thionyl chloride containing a drop of DMF were reacted until the solution became clear (approximately 3 h). The excess thionyl chloride was removed by a vacuum rotary evaporator to obtain yellow, viscous 4-allyloxybenzoyl chloride. The acid chloride was dissolved in 5 mL CH_2Cl_2 and slowly added to a solution of 0.019 mol (5.47 g) intermediate compound IBE2DB containing excess dry triethylamine in 50 mL of CH_2Cl_2 in ice water to incur reaction. CH_2Cl_2 and triethylamine in the reaction solution were removed by the rotary evaporator under reduced pressure. The residual material was purified in a silica gel packed column with CH_2Cl_2/*n*-hexane/methanol (20 v/5 v/1 v) as the mobile phase to obtain 6.38 g of pure product (yield 75%); MS3BE1DB : CH_2Cl_2/*n*-hexane/methanol (40 v/10 v/1 v) was the mobile phase (yield 78%). MS3BE3DB : CH_2Cl_2/*n*-hexane/methanol (40 v/10 v/3 v) was the mobile phase (yield 65%). MS8BE2DB : CH_2Cl_2/*n*-hexane/methanol (40 v/10 v/1 v) was the mobile phase (yield 52%). The characteristic ^{1}H-NMR and ^{13}C-NMR chemical shifts of the monomer MS3BDBE*n* are respectively summarized in Tables I and II.

Synthesis of Polymers

All the polymers in this study were synthesized according to the procedure of Chang-Chien et al.[15] The monomer-grafted reactions were carried out in toluene with the Pt-catalyzed hydrosilylation process. Completion of reaction (approximately 24 h) was monitored by the disappearance of the Si—H absorption peak. Repeated precipitation from dichloromethane with methanol was followed by vacuum drying of the polymers at room temperature. The PS3BDBE0 and PS3BDBE1 polymers were not easily dissolved in toluene and precipitated during the graft reaction. The collected rough polymers PS3BDBE0 and PS3BDBE1, which were precipitated in methanol, also did not easily dissolve in

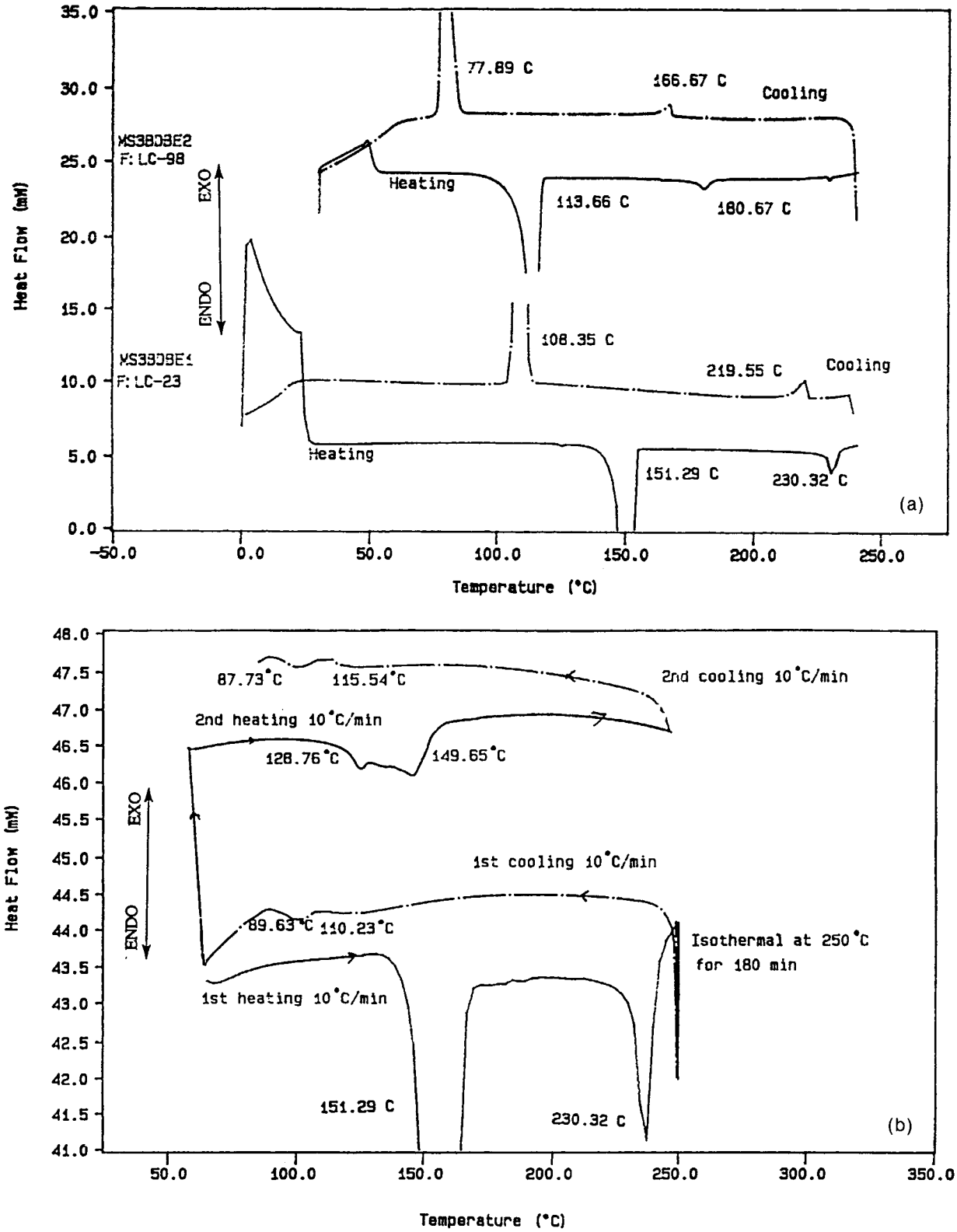

Figure 4 DSC thermograms of the monomers MS3-BDBE0, MS3BDBE1, MS3BDBE2 (heating and cooling rate of 10°C/min). (a) MS3BDBE1 and MS3BDBE2, (b) monomer MS3BDBE1 with isothermal annealing at 250°C for 180 min, (c) monomer MS3BDBE0 in a repeated heating and cooling experiment.

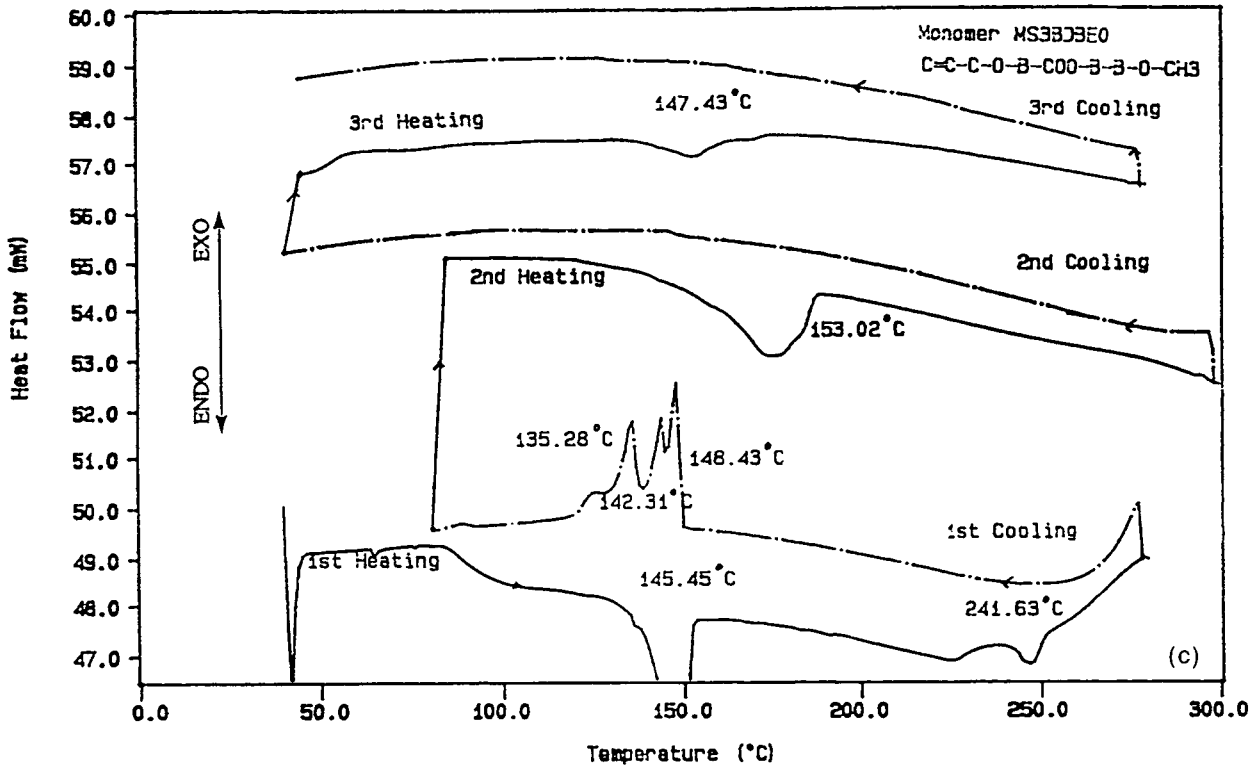

Figure 4. (*Continued from the previous page*)

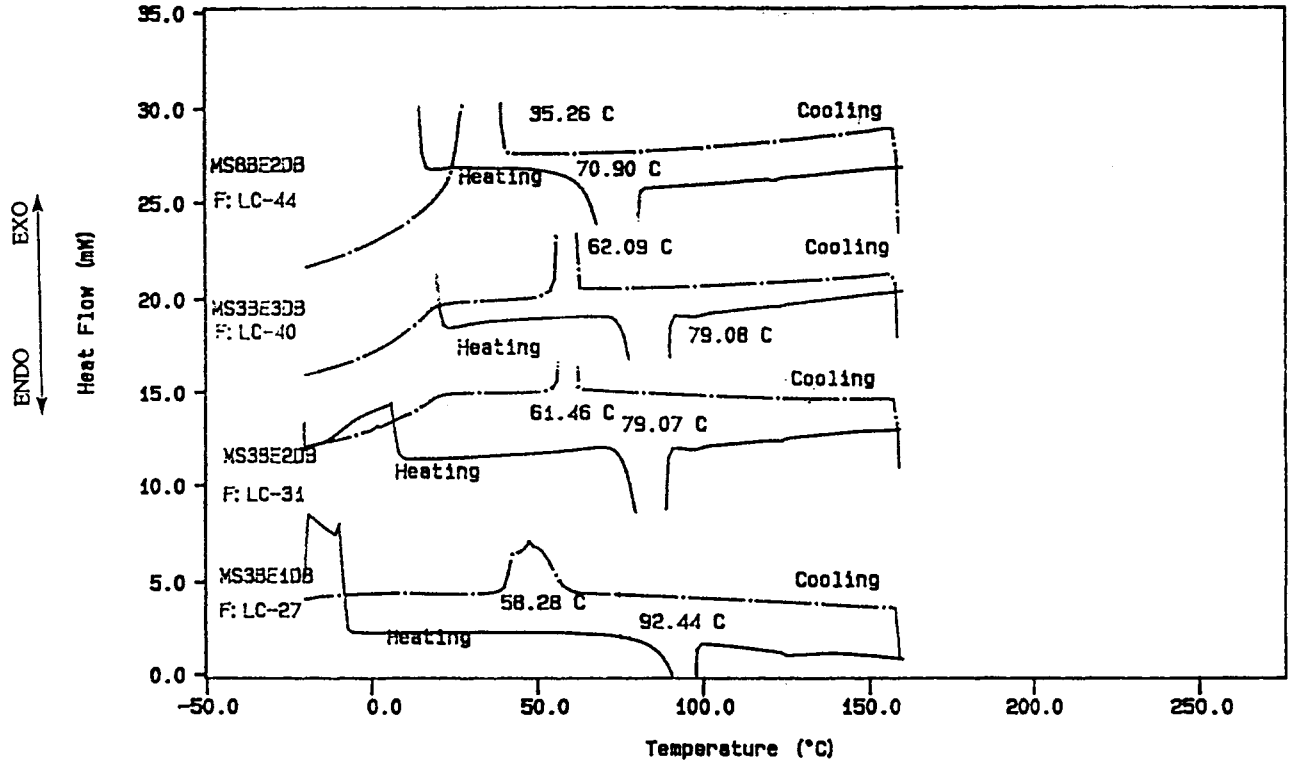

Figure 5 DSC thermograms of the monomers MS3-BE1DB, MS3BE2DB, MS3BE3DB, and MS8BE2DB (heating and cooling rate of 10°C/min).

dichloromethane. So these grafted polymers were purified by hot methanol washed.

RESULTS AND DISCUSSION

Schemes 1 and 2 outline the procedures used to prepare the intermediate compounds, monomers, and side-chain polysiloxane polymers. The purified products in this study were confirmed by thin-layer chromatography and then were further characterized by ^{1}H-NMR and two-dimensional NMR spectra.[24] The thin-layer chromatography diagram only showed one spot in a 254 cm^{-1} wavelength ultraviolet (UV) light with CH_2Cl_2/*n*-hexane/methanol solvent system as the mobile phase at different compositions. Figure 1 illustrates the 200-MHz ^{1}H-NMR spectra of the monomers MS3BDBE1 and MS3BE2DB. Table I summarizes the chemical shifts of characteristic groups of the monomers. The relative peak areas of the assigned chemical shifts are in agreement with expected values from the molecular structure. Figures 2(a), (b), (c), (d), (e), and (f) respectively illustrate the ^{13}C-NMR, DEPT-135, HMBC, HMQC, and COSY 90 spectra of MS3BE2DB. Table II summarizes the carbon chemical shifts of the monomers in this study.

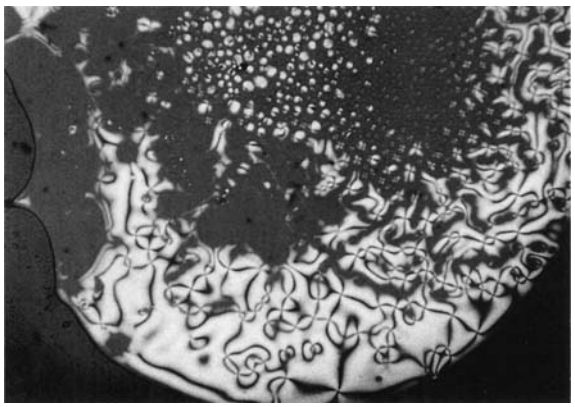

Figure 6 Polarized optical microscope presenting the nematic schlieren texture of monomer MS3BDBE1 at 175°C (cooling scan).

All the monomers discussed and compared in this study are of three types based on molecular structure. The first type[15] which had been discussed previously

Table III Thermal Transition Temperature (°C)[a] Mesophase Types,[b,c] and Thermodynamic Parameters[d] for the Monomers in This Study

Monomers	Cooling / Heating
ME1S3[e]	K 107.02 S_A 151 (1.62/3.82) N 180 (0.63/1.39) I
	I 173.34 (0.56/1.25) N 144.43 (1.53/3.66) SA 79 K
ME2S3[e]	K 91.32 S_A 146 (2.57/6.13) N 157 (0.51/1.19) I
	I 155 (0.51/1.19) N 143 (2.33/6.00) S_A 65 K
MS3BDBEO[f]	K 145.46 N 247.96 (5.41/10.4) I
	148.43, 142.31, 135.28 K
MS3BDBE1	K 151.29 N 230.32 (4.92/9.77) I
	I 219.55 (2.95/5.99) N 108.35 I
MS3BDBE2	K 113.66 N 180.67 (2.06/4.54) I
	I 166.67 (1.62/3.68) N 77.89 K
MS3BE1DB	K 92.44
	58.28 I
MS3BE2DB	K 79.07
	61.46 K
MS3BE3DB	K 79.08
	62.09 K
MS8BE2DB	K 70.90
	35.26 K

[a] Heating and cooling rates were 10°C/min.
[b] Mesophase types were determined by polarized optical microscopy.
[c] K: crystalline; SA: smectic phase A; N: nematic phase.
[d] Thermodynamic parameters [ΔH(J/g)/ΔS(J/kg°C)].
[e] Ref. 15.
[f] The results reported by M. A. Apfel et al.[22] were (K 147°C N 249°C I).

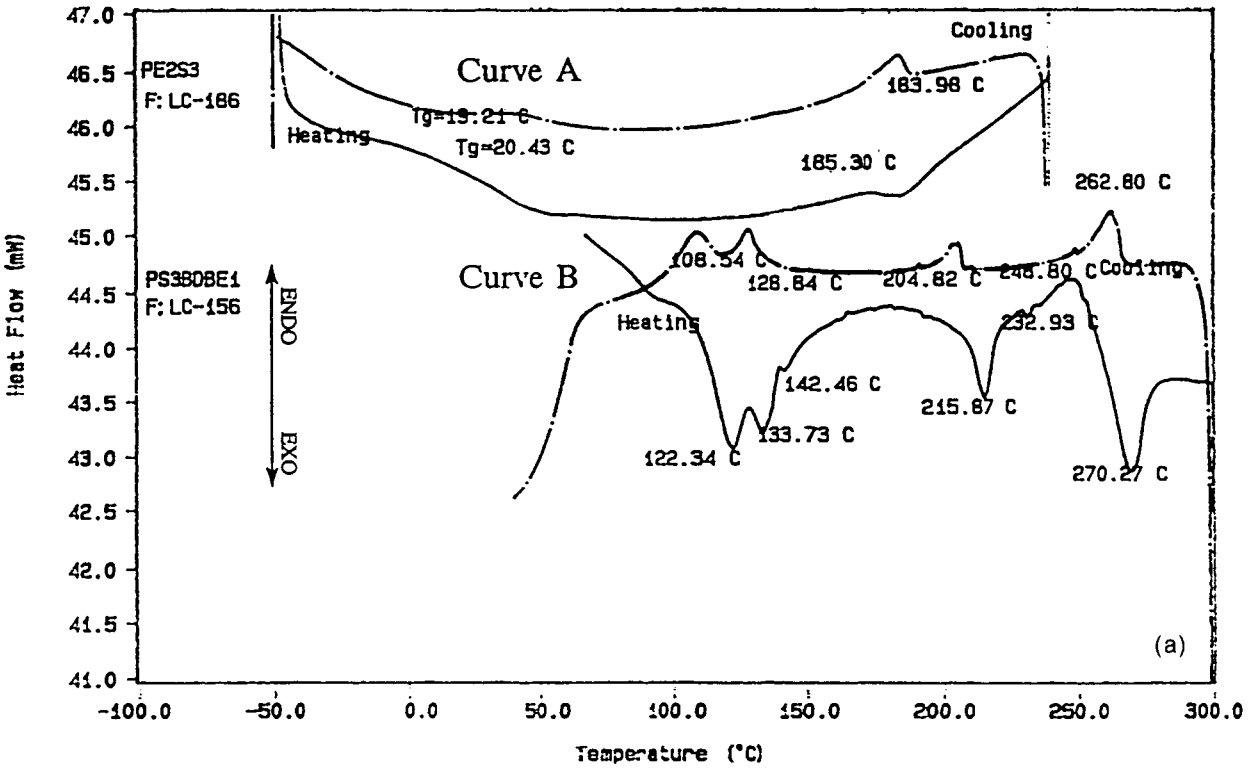

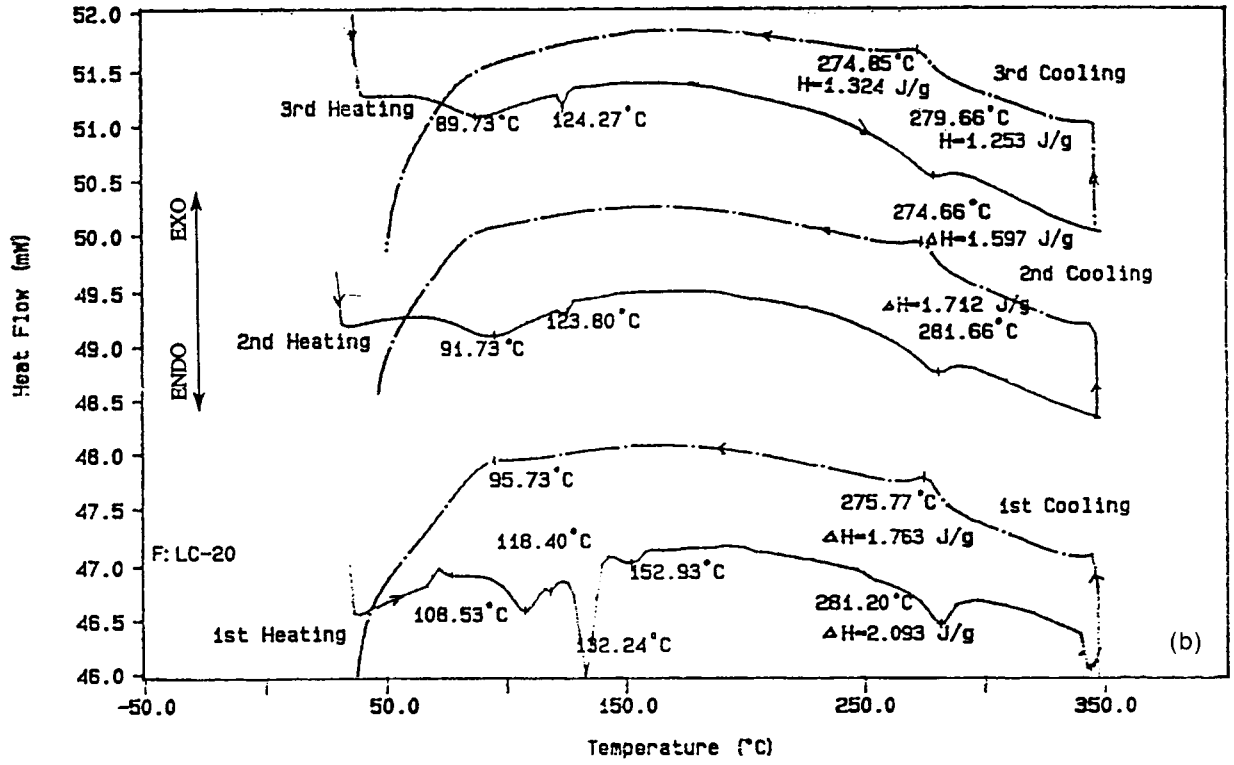

Figure 7 DSC thermograms of the polymers (a) PS3E2 and PS3BDBE1, (b) PS3BDBE0, and (c) PS3BDBE2 (heating and cooling rate of 10°C/min).

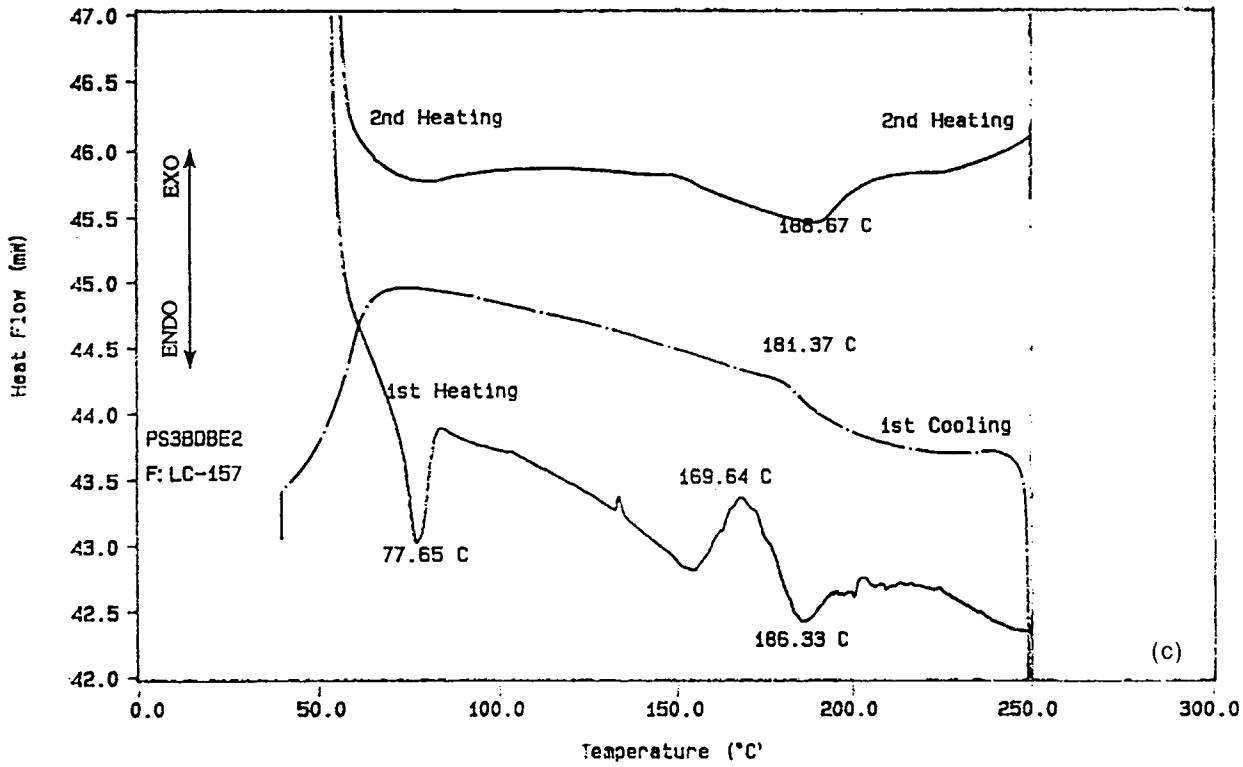

Figure 7. *(Continued from the previous page)*

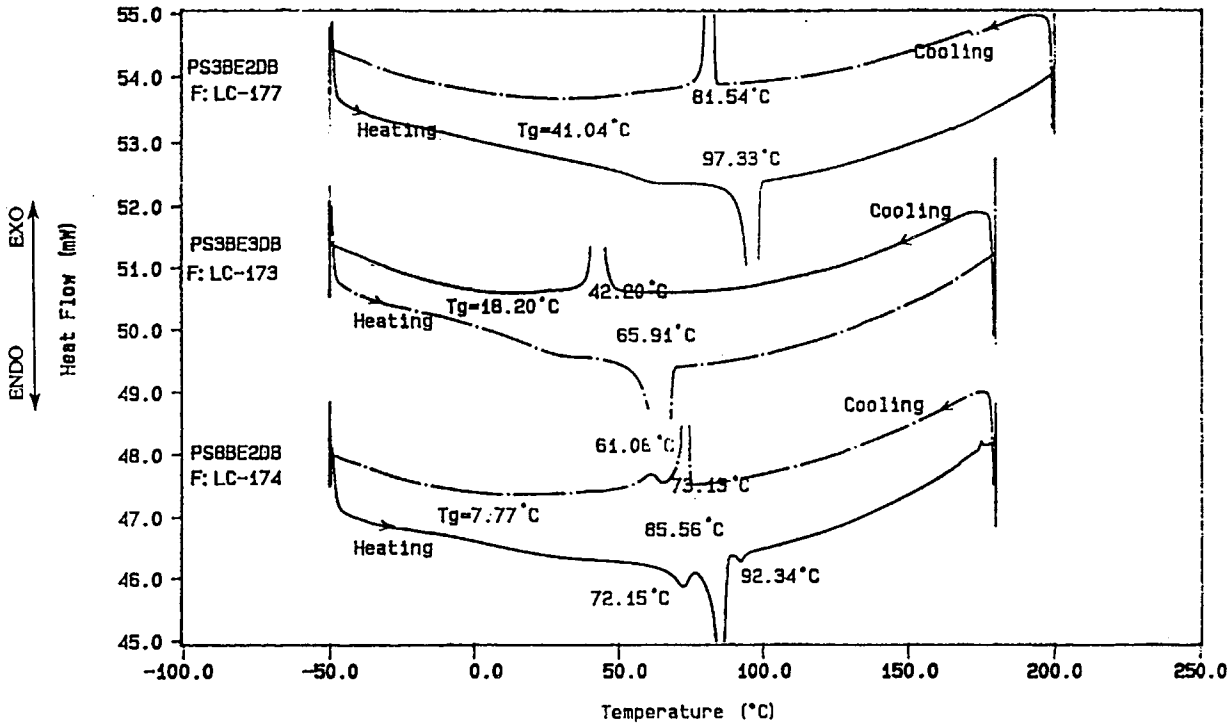

Figure 8 DSC thermograms of the polymers PS3-BE2DB, PS3BE3DB, and PS8BE2DB (heating and cooling rate of 10°C/min).

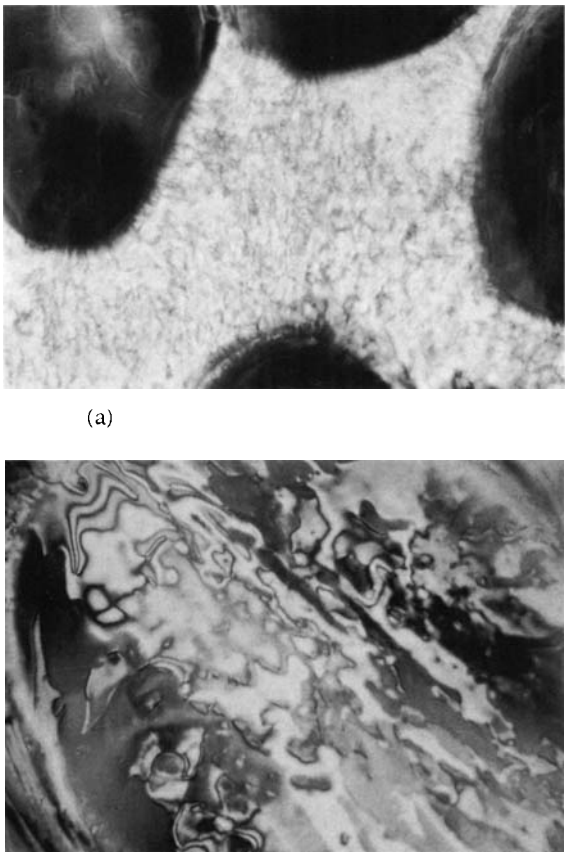

(a)

(b)

Figure 9 Polarized optical micrographs presenting (a) smectic texture (145°C) and (b) nematic schlieren texture (210°C) of polymer PS3BDBE1 (cooling scan).

had a "carboxyl" linkage between the mesogenic core and a mono- or di(ethylene oxide) monomethyl ether terminal group (i.e., ME1S3 and ME2S3). The second type had an "ether" linkage between the mesogenic core and terminal group of oligo(ethylene oxide) (i.e., MS3BDBE1 and MS3BDBE2). The third type had a flexible oligo(ethylene oxide) group as a linkage between the carboxyl benzoate group and the biphenyl group (i.e., MS3BE1DB, MS3BE2DB, MS3BE3DB, and MS8BE2DB).

Figures 3 to 5 show the differential scanning calorimetry (DSC) thermograms of the monomers in this study. The transition temperatures and thermodynamics parameters are summarized in Table III. Monomers ME1S3 and ME2S3 exhibited both the smectic and nematic phase.[15] The length of the ethylene glycol monomethyl ether terminal group influenced the thermal transition behavior and the change of enthalpy and entropy. The longer the oligo(ethylene oxide) unit, the lower the smectic and nematic phase transition temperatures. For the smectic phase, the monomer ME2S3, which has the longest oligo(ethylene oxide), had the largest changes of enthalpy and entropy. In contrast to the smectic phase, the ME2S3 monomer nematic transition had the smallest changes of enthalpy and entropy and a narrower nematic mesophase transition temperature range. Obviously, the increased length of the terminal group was favorable to the smectic phase.

Figure 3 shows the change of mesophase transition temperatures for ME2S3 with several heating and cooling scans. The temperature ranges of the smectic phase and nematic phase were, respectively, 59.65°C (145.97°C ~ 86.32°C) and 11.24°C (157.21°C ~ 145.97°C) for the first heating scan, 80.82°C (53.49°C ~ 134.82°C) and 17.23°C (134.82°C ~ 151.54°C) for the first cooling scan, 53.03°C (81.42°C ~ 134.45°C) and 19.85°C (134.45°C ~ 154.30°C) for the second heating, 78.91°C (45.65°C ~ 124.56°C) and 24.27°C (124.56°C ~ 148.83°C) for the second cooling, 49.54°C (77.56°C ~ 127.10°C) and 25.64°C (127.10°C ~ 152.74°C) for the third heating, and 73.95°C (45.09°C ~ 119.04°C) and 29.29°C (119.04°C ~ 148.33°C) for the third cooling. The smectic phase temperature range decreased with increasing scans in contrast to the nematic phase temperature range, which increased.

Figure 4(a) shows the heating and cooling DSC thermogram for the monomers MS3BDBE1 and MS3BDBE2. Figure 5 illustrates the typical nematic schlieren texture of MS3BDBE1. The transition temperatures and thermodynamic parameters are listed in Table III. For the monomers MS3BDBE1, MS3BDBE2, ME1S3, and ME2S3, one finds that when the "ester" linkage in the monomers ME1S3 and ME2S3 was replaced with an "ether" linkage having the same chain length of oligo(ethylene oxide) as MS3BDBE1 and MS3BDBE2, respectively, the smectic phase disappeared and the nematic phase transition temperatures (T_{Ni}) became higher and more widely spaced. The ether oligo(ethylene oxide) length influenced the nematic thermal transition behavior and the change of enthalpy and entropy. The longer the oligo(ethylene oxide) unit, the lower the nematic phase transition temperature. Figure 4(b) shows the thermal behavior of the MS3BDBE1 after annealing at 250°C for 20 min. No nematic transition peak is observed, and the crystal melting peak becomes more wider with multiple peak.

Monomers MS3BDBE0, MS3BDBE1, and MS3BDBE2 have the same mesogenic core and alkenyloxy group but different terminal groups. Figure

Table IV Thermal Transition Temperature (°C)[a] Mesophase Types[b,c] and Thermodynamic Parameters[d] for the Polymers in This Study

Monomers	Cooling / Heating
PE1S3[e]	Tg 29 S 251 (2.29/4.40) I I 248 (1.80/3.45)
PE2S3[e]	Tg 22 S 187 (2.21/4.80) I I 184 (2.30/5.03)
PS3BDBE0[f]	K 108.53, 118.40, 132.24, 152.93 N 281.20[d] (2.09/3.77) I I 275.77 (1.76/3.21)
PS3BDBE1	K 122.34, 133.73, 142.46 S, 215.87 N 270.27 I I 262.80 N 204.82 S 128.84, 108.54 K
PS3BDBE2	K 77.65 S 169.64 N 186.33 I I 186.67 N
PS3BE1DB	Tg 38.59 K 81.08 72.23 I
PS3BE2DB	Tg 41.04 K 97.33 81.54 K
PS3BE3DB	Tg 18.20 K 65.91 42.20 K
PS8BE2DB	Tg 7.77 K 85.56 73.15 K

[a] Heating and cooling rates were 10°C/min.
[b] Mesophase types were determined polarized optical microscopy.
[c] K: crystalline; SA; smectic phase A; N: nematic phase.
[d] Thermodynamic parameters [ΔH(J/g)/ΔS(J/kg°C)].
[e] Ref. 15.
[f] The nematic transition temperature (T_{Ni}) was 319°C, which was reported by M. A. Apfel et al.[22]

4(c) shows the repeated heating and cooling DSC thermograms of MS3BDBE0. The transition temperature and thermodynamic parameters are listed in Table III. The transition temperatures (K 145.45°C N 247.63°C I) of the first heating scan approach the results (K 147°C N 249°C I) reported by Apfel et al.[22] However, after the monomer MS3BDBE0 was held at 280°C for a few minutes, three crystal transitions (148.43°C, 142.31°C, and 135.28°C) occured upon cooling. Instead of the melting at 145.45°C as in the first heating curve, a wider endothermic peak (135.27°C ~ 175.45°C) (possibly with multiple peaks) is obtained with the second heating scan. The intensity of the peak became gradually smaller with subsequent scans. Obviously, the monomer MS3BDBE0 decomposed at temperatures above the isotropic temperature.

Figure 6 shows DSC thermograms of monomers MS3BE1DB, MS3BE2DB, MS3BE3DB, and MS8BE2DB. The transition temperatures and thermodynamic parameters are listed in Table III. The molecular structure of these monomers is similar to MS3BDBE0, except that one, two, or three units of the oligo(ethylene oxide) group connect the carboxyl benzoate group and biphenyl group. From the DSC thermograms and polarized optical microscopy, the monomers MSm+2BEnDB(m = 1,6; n = 1 to 3) showed no mesophase behavior. Obviously, a flexible oligo(ethylene oxide) group incorporated into the carboxyl benzoate and biphenyl group would strongly depress formation of the mesophase. A low molar mass liquid crystal presented only monotropic or virtual transitions[19-21] when methyleneoxy or ethane groups were interconnecting units between two phenyl rings.

The polymers in Table IV were obtained by grafting the monomers listed in Table III onto PMHS by the Pt-catalyzed hydrosilylation process. Differential scanning calorimetry thermograms of the polymers are shown in Figures 7 and 8. Figures 9(a) and (b) illustrate the typical smectic texture and nematic schlieren texture of PS3BDBE1 from the polarized optical microscope. Table IV sum-

marizes the transition temperature, thermodynamic parameters, and mesophase type of the polymers. PE1S3 and PE2S3 showed a smectic phase with titled two-layer packing determined by the polarized optical microscope and X-ray diffraction method.[15,16] The mesophase type and transition temperature of polymers PE1S3 and PE2S3 were not analogous to those of their precursor monomers even though their precursor monomers showed both the smectic and nematic phase. Figure 7(a) illustrates the DSC thermograms of the polymers PE2S3 and PS3BDBE1. The polymer PE2S3 DSC thermograms [Fig. 7(a), curve A] shows a T_g at 20.43°C and a T_{si} at 185.30°C in a first heating, followed by annealing at 230°C for 180 min, and then cooling from 230°C to −50°C. We found that the polymer PE2S3 did not decompose for long annealing times above the isotropic temperature.

Figures 7(b) and (c), respectively, illustrate the DSC thermograms for the polymers PS3BDBE0 and PS3BDBE2. The transition temperatures and thermodynamic parameters also listed in Table IV. The PS3BDBE0 polymer nematic transition (T_{Ni}) temperature of 281.54°C was lower than the value 319°C, which was reported by Apfel et al.[22] Figure 7(a) shows three crystal melting points at 122.34°C, 133.73°C, and 142.46°C; three mesophase transition temperatures at 215.87°C, 232.93°C, and 270.27°C; and, upon cooling from 300°C, two mesophase transition temperatures at 262.80°C and 204.82°C and two crystallization points at 128.84°C and 108.54°C. The isotropic temperature of the PS3BDBE*n* polymer decreased as the terminating oligo(ethylene oxide) lengths increased, similar to the polymers PE1S3 and PE2S3. This conflicts with results reported by Janini et al.,[23] which indicated that a methoxy biphenyl side chain had a much higher isotropization temperature than the corresponding polymer with a biphenyl side chain.

Figure 8 show the DSC thermograms of PS3BE2DB, PS3BE3DB, and PS8BE2DB, respectively. We could not find any mesophase transition endothermic peaks. None of the aforementioned polymers shows any characteristic mesophase texture in the polarized optical microscope. The PS*m*+2BE*n*DB polymers were similar to PS3BDBE0 except for an oligo(ethylene oxide) unit between the carboxyl benzoate and biphenyl groups. Obviously, since the molecule with a flexible oligo(ethylene oxide) unit as an interconnection unit between the carboxyl benzoate and biphenyl did not give rise to a thermally stable mesophase, its attachment was as a side group to a polysiloxane backbone. This result was not similar to the acrylate and methacrylate polymers containing *p*-cyanophenyl-*p*-hydroxybenzyl ether, *p*-methoxyphenyl-*p*-hydroxybenzyl ether, and 1-(*p*-cyanophenyl)-2-(*p*-hydroxyphenyl)ether groups which exhibited enantiotropic mesomorphism reported by Hsu and Percec.[19] For a flexible oligo (ethylene oxide) connection between a carboxyl benzoate and diphenyl group, the instability of the mesogenic unit is likely caused by the motion of the flexible oligo(ethylene oxide) and is not overcome by constraints generated from the polymer chains so that anisotropic ordering of mesogens is not attained.

CONCLUSION

The linkage group profoundly affects the mesophase type, thermal transition temperature, and thermal behavior. The melting point and the transition temperature with the "ether" linkage were higher than with the "ester" linkage. Both "ether" and "ester" linkage polymers of the mesophase type are not similar to their polymeric homologues. A flexible oligo(ethylene oxide) unit inserted between the carboxyl benzoate group and biphenyl group was unfavorable to the formation of a mesophase for monomers and their side-chain polysiloxane polymers.

We thank Dr. Shiun and Ru-Zong Wu for their help in carrying out the NMR spectra measurements. We also thank Micheal Gentzler and Professor Morton M. Denn for reading the manuscript and making many helpful suggestions. Financial support from the National Science Council of the Republic of China (NSC-83-0117-C-230-001E) is gratefully acknowledged.

References

1. H. Finkelmann, H. Ringsdorf, and J. H. Wendorff, *Makromol. Chem.*, **179,** 273 (1978).
2. C. S. Hsu and V. Percec, *Makromol. Chem. Rapid Comm.*, **8,** 331 (1987).
3. H. Gingsdorf and A. Schneller, *Makromol. Chem. Rapid Comm.*, **3,** 557 (1982).
4. J. M. Rodriguez–Parada and V. Percec, *J. Polym. Sci.*, **24,** 1363 (1986).
5. H. J. Coles and R. Simon, *Polymer,* **26,** 1801 (1985).
6. V. P. Shibaev, S. A. Ivanov, S. G. Kostromin, N. A. Plate, V. Y. Vetrov, and I. A. Yakovlev, *Polymer Communications,* **24,** 364 (1983).

7. C. B. Mcardle, M. G. Clark, G. W. Gray, C. M. Haws, D. Lacey, G. Nestor, A. Parker, K. J. Toyne, and M. C. K. Wiltshire, *J. Liq. Cryst.*, **2,** 573 (1987).
8. H. Finkelmann and G. Rehage, *Makromol. Chem. Rapid Commun.*, **3,** 859 (1982).
9. H.-J. Eberle, A. Miller, and F.-H. Kreuzer, *J. Liq. Cryst.*, **5,** 907 (1989).
10. M. F. Bone, G. W. Gray, D. Lacey, P. A. Gemmell, K. J. Toyne, L. K. M. Chan, D. Coates, J. Constant, and M. J. Bradshaw, *Mol. Cryst. Liq. Cryst.*, **164,** 117 (1988).
11. B. A. Jones, J. S. Bradshaw, M. L. Lee, and M. Nishioka, *J. Org. Chem.*, **49,** 4947 (1984).
12. J. E. Haky and G. M. Muschik, *J. Chromatogr.*, **214,** 161 (1981).
13. S. K. Varshney, *J. Macromol. Sci. Rev. Macromol. Chem. Physics,* **6,** 551 (1986).
14. G. W. Gray, W. D. Hawthorne, J. S. Hill, M. S. White, G. Nestor, D. Lacey, and M. S. K. Lee, *Polymer,* **30,** 946 (1989).
15. G.-P. Chang-Chien, J.-F. Kuo, and C.-Y. Chen, *J. Polym. Sci.*, **31,** 2423 (1993).
16. G.-P. Cheng-Jeng, J.-F. Kuo, and C.-Y. Chen, *J. Appl. Polym. Sci.*, **47,** 697 (1993).
17. G.-P. Chang-Chien, J.-F. Kuo, and C.-Y. Chen, *J. Appl. Polym. Sci.*, **47,** 781 (1993).
18. D. Demus and L. Richter, *Texture of Liquid Crystals,* VEB Deutscher Verlag der Wissenschaften, Leipzig, 1980, p. 6.
19. C. S. Hsu and V. Percec, *J. Polym. Sci.*, **27,** 453 (1989).
20. N. Carr and G. W. Gray, *Mol. Cryst. Liq. Cryst.*, **124,** 27 (1985).
21. N. H. Tinh, H. Gasparoux, and C. Destrade, *Mol. Cryst. Liq. Cryst.*, **123,** 271 (1985).
22. M. A. Apfel, H. Finkelman, T. J. Shaw, C. A. Smith, W. L. Roberts, A. Price, B. H. Luhmann, R. J. Laub, and G. M. Janini, *Anal. Chem.*, **57,** 651 (1985).
23. G. M. Janini and R. J. Shaw, *Makromol. Chem. Rapid Commun.*, **6,** 57 (1985).
24. M. F. Summers, A. Bax, and L. G. Marzilli, *J. Am. Chem. Soc.*, **108,** 4285 (1986).

Received July 15, 1994
Accepted November 12, 1994